Comparative Biochemistry and Physiology - Part D: Genomics and Proteomics 47 (2023) 101103

Contents lists available at ScienceDirect

Comparative Biochemistry and Physiology - Part D: Genomics and Proteomics

journal homepage: www.elsevier.com/locate/cbpd

Using proteomics, q-PCR and biochemical methods complementing as a multiapproach to elicit the crucial responses of zebrafish liver exposed to neonicotinoid pesticide

Seyma Kizilkaya [a,*], Gurler Akpinar [b], Nuzhet Cenk Sesal [c], Murat Kasap [b], Baris Gokalsin [c], Figen Esin Kayhan [c]

[a] Marmara University Institute of Pure and Applied Sciences, Istanbul 34722, Turkiye
[b] Kocaeli University Faculty of Medicine, Department of Medical Biology, Kocaeli 41001, Turkiye
[c] Marmara University Faculty of Science, Department of Biology, Istanbul 34722, Turkiye

ARTICLE INFO

Edited by Chris Martyniuk

Keywords:
Proteomics
q-PCR
Pesticide
Enzymatic activity
Gene expression
Zebrafish
Liver
CAT
GSH
AChE
MDA
cat
gpx
ache
pxr
Model organism
Neonicotinoid
Imidacloprid

ABSTRACT

Pesticides enter the environment through runoff and leaching and this raises public concern about effects on non-target organisms. Imidacloprid (IMI) a synthetic pesticide, has an unstable half-life, metabolized in minutes to weeks in the water. To evaluate the effects of IMI on the zebrafish liver, we conducted proteomic, molecular and biochemical analysis in a multi-level approach, to highlight the complementary features regarding the results of each method. Adult zebrafish were exposed to 60 mg/L IMI for 48 h and were evaluated using nLC-MS/MS for proteins, q-PCR analysis for expression of *cat*, *gpx*, *pxr*, *ache*, along with CAT and AChE enzyme activities and GSH and MDA assays. Based on proteomics, the regulation of antioxidant and immune responses, as well as gene transcription were significant processes affected. Apoptosis and ER stress pathways were upregulated and there was a down-regulation of *cat* and *gpx* genes. There was also elevated CAT activity and GSH and decreased MDA. Additionally, elevated AChE activity and up regulation of ache expression was observed. The multi-approach results included regulators of antioxidant, xenobiotic response and neuro-protective related proteins (genes and enzymes), which overall reflected harmful effects of IMI. Consequently, this study highlights the effects of IMI on zebrafish liver and reveals new potential biomarkers. In this respect, evaluated outcomes reveal the complementary features emphasizing the importance of studying chemicals using several methods. Our study provides deeper insights for future work in ecotoxicological studies regarding IMI and contribute to existing toxicity literature.

1. Introduction

Environmental sensitivity is extensively common; to evaluate pollutant effects, particularly on nontarget organisms, a single approach is not adequate, and a multiple approach is needed. Ecotoxicological studies are designed to evaluate how environmental pollutants affect nontarget organisms to support policies that protect humans and wildlife (Groh and Suter, 2015a). These pollutants generate persistent and severe ecological problems and consequently cause public concern (Wang et al., 2017; Zhang et al., 2021; Luo et al., 2021c; Bruckmann et al., 2022). In agricultural applications, neonicotinoid insecticides are the most widely used synthetic pesticides (Topal et al., 2017a). During agricultural activities, it is possible to encounter accidents, misusages, spills and/or leakages. Widespread pesticide applications in agricultural areas, as these pollutants are introduced into the environment via runoff and leaching, are emerging as a threat to the ecological balance in aquatic environments (Topal et al., 2017a; Esin Kayhan et al., 2019). Imidacloprid (IMI) is a frequently used insecticide, and its principal characteristic is acting as a nicotinic acetylcholine receptor (nAChR) agonist that targets cholinergic neurotransmission (Luo et al., 2021c).

* Corresponding author.
E-mail addresses: seymat@gmail.com, seymatartar@marun.edu.tr (S. Kizilkaya).

https://doi.org/10.1016/j.cbd.2023.101103
Received 9 January 2023; Received in revised form 10 June 2023; Accepted 10 June 2023
Available online 15 June 2023
1744-117X/© 2023 Elsevier Inc. All rights reserved.

IMI has a relatively long half-life in soil (Bonmatin et al., 2015; Thunnissen et al., 2020), high water solubility (610 mg/L in 20 °C H_2O; log Kow = 0.57) and high potential to reach water (Nyman et al., 2013). Consequently, in aqueous samples, imidacloprid is reasonably stable to hydrolysis at environmentally relevant pH values (Yoshida, 1989) yet undergoes rapid photolytic degradation (Tišler et al., 2009). As an important feature, following IMI reaching the water bodies, the dissipation time of 50 % (DT50) of IMI solely relies on photolysis and was reported as 1.2 days (although it ranges (Smit and De Jong, 2014). Hence, it has the potential to accumulate in soils and leach to surface water and groundwater (Hladik et al., 2018). Moreover, current studies have revealed detected IMI concentrations of up to 320 μg/L worldwide in the Netherlands close to agricultural areas (Van Dijk et al., 2013; Morrissey et al., 2015). The reported estimated values of accidental spill-off and/or leakages were 1.8 to 7.3 mg/L (N W Thunnissen et al., 2020), and the measured surface water concentrations were 14 μg L^{-1} to 0.3 mg L^{-1} (Wu et al., 2018a) Altogether, these characteristics result in nontarget freshwater organisms being easily exposed and adversely affected by IMI (Thunnissen et al., 2020). Likewise, previous studies proved the existence of IMI residuals in water bodies, thus possibly causing various adverse effects on nontarget aquatic organisms (Anderson et al., 2015; Morrissey et al., 2015; Struger et al., 2017; Thunnissen et al., 2020; Luo et al., 2021c).

These pollutants (insecticides) stimulate oxidative stress by constituting reactive oxygen species (ROS), followed by oxidative damage and significant damage to cell structures (Zhu et al., 2023). Moreover, they affect macromolecules, which leads to oxidative damage in nucleic acids, lipids, and proteins (Topal et al., 2017b; Zhang et al., 2018).

Zebrafish are frequently used to evaluate the adverse effects of pesticides due to their easy care, low cost, small size, susceptibility to environmental alterations, and high genomic similarities to human genes (Li et al., 2022). Furthermore, zebrafish is recommended as an essential biological model by the Organization for Economic Cooperation and Development (OECD) (OECD, 1992; McGrath and Li, 2008; Li et al., 2022). The fish liver is a decisive organ for systemic regulation and a principal organ for detoxification to eliminate pathogens, toxic substances, and metabolic wastes, along with sustaining the physiological functions (Chen et al., 2017) used in toxicology studies.

Previous studies have promoted biochemical (mostly enzymatic such as catalase (CAT), acetylcholinesterase (AChE) but also malondialdehyde (MDA) and glutathione (GSH) content responses) and molecular (gene expression alterations) analyses to investigate and highlight the adverse effects of pesticides. Likewise, recent studies of IMI adverse effects assessment on zebrafish have focused mainly on evaluating the responses via biochemical (Shukla et al., 2017a; Kayhan et al., 2020; Guerra et al., 2021; Queiroz et al., 2021) and molecular approaches (Sposito et al., 2018; Zhang et al., 2021) and both (Luo et al., 2021a, 2021c). Nevertheless, as a recently preferred approach, Reinwald et al. (2022) investigated the effects of IMI with several other pesticides by toxicogenomic profiling. Nevertheless, observations of IMI-responsive protein functions and knowledge of whether they function consistently during the stress process are absent. Nevertheless, frequently preferred approaches do not render the intricacy of the cell response that is a combination of alterations in protein expression and controlled post-translational modifications of proteins (Zhang et al., 2017). However, proteomics has the advantage of ensuring details about protein abundances, stabilities, turnover rates, posttranslational modifications, and protein–protein interactions, consequently conveying precise and reviewed information (Groh and Suter, 2015a). Proteins are the most prominent in vivo targets of oxidants, with almost 70 % of all oxidized molecules being proteinaceous in oxidatively stressed cells (Truong and Carroll, 2013). Because proteomics can provide itemized data on protein quantity, stability, revolution speed, posttranslational modifications, and protein–protein interactions (Groh and Suter, 2015a), we first focused on proteomic outcomes.

The data mining studies indicated a lack and need for complementary analyses and multiapproach experience throughout the evaluation of the effects of IMI on zebrafish liver. To date, the effects of IMI have not been studied via proteomic approaches, and this study is the first to evaluate these effects. In addition to the advantageous features of the proteomic approach, integrating/complementing it with the other two, molecular and biochemical approaches would strengthen the insight into the responses of organisms to environmental pesticides. To test the links between the effects of insecticide exposure on the zebrafish liver proteome, transcript, and activity levels of the specific components of the oxidative stress response, we focused on an experimental design comprised of multiapproach analyses. We anticipate that this model will contribute to filling the knowledge gap regarding the limits of pesticide effects. This study's objective was to add profound insights into pesticide-IMI effects on the nontarget organism's zebrafish liver by conducting a multiapproach comprised of proteomic, molecular, and biochemical complementary analyses.

2. Materials and methods

2.1. Zebrafish maintenance and experimental design

Healthy adult zebrafish (*Danio rerio*) weighing between 0.25 g and 0.30 g were purchased from a regional supplier and acclimatized to a 28 ± 1 °C aquarium with a photoperiod of 12:12 h (light-dark) while fed commercial food (Tetrabits Complete, Germany) twice a day and with freshly hatched *Artemia nauplii* once a day for two weeks. Water was changed daily to dispose of metabolic waste. The rules of the "Marmara University Institutional Animal Ethics Committee" were applied while experiments were carried out to sustain the welfare of the subjected animals.

Ecotoxicological studies observing the effects of IMI previously reported LC50 values of IMI for adult zebrafish 48 h acute exposure as 305.43 (288.93–333.14) mg a.i. L^{-1} (Chang et al., 2020), 186,900 μg/L (Thunnissen et al., 2020). Moreover, Tišler et al. (2009) tested a range of acute exposure concentrations for 24 and 48 h (10, 40, 60, 80, 160, and 320 mg L^{-1}) and stated that the solution stability of IMI did not change up to 70 mg L^{-1} during 22 days of exposure. In addition, following IMI reaching the water bodies, although it ranges (Smit and De Jong, 2014), the dissipation time of 50 % (DT50) of IMI solely relies on photolysis and is reported as 1.2 days from the monitored water column (Colombo et al., 2013; Smit and De Jong, 2014). Based on the abovementioned studies and literature review (Scheil and Köhler, 2009; Tišler et al., 2009; Wu et al., 2018a; Chang et al., 2020; Thunnissen et al., 2020; Luo et al., 2021a; Reinwald et al., 2022), we chose the sublethal test concentration as 60 mg/L for 48 h. Furthermore, we tested the 60 mg/L concentration for 48 h exposure and observed no mortality. In this study, we note that our aim was not to quantify the LC50 and/or EC50 concentration values of IMI but to gain information about the effects of relatively high sublethal concentrations of the mentioned pesticide.

After the acclimatization period, zebrafish were randomly divided into two groups (30 fish each) of IMI treatment and control. The fish were maintained in 10 L tanks with a stocking density of 3 fish/L. The stock solution was freshly prepared in aquarium water as a 1:10 serial dilution to 60 mg/L and stirred at 20 °C. As soon as the exposure period finished, we dissected the adult fish on ice and placed the tissues in tubes that were on dry ice. Afterward, we immersed the sample tubes in liquid nitrogen for a very short time, placed them in a freezer at −80 °C and stored them until the experiments were carried out. The same protocol was applied to control adult fish. During the exposure duration, no fish mortality was observed.

2.2. Proteomic analysis

2.2.1. Protein extraction and pooled sample preparation

The proteomics experiments were performed with three biological pooled samples, with each pool containing three zebrafish livers (n = 9)

and two technical replicates (for the control and treated groups). Sample preparation was conducted with respect to prior studies (Simsek et al., 2022) with minor modifications. In short, the biological pooled replicates of treated and untreated groups of zebrafish liver samples were transferred into precooled Eppendorf tubes and centrifuged at 4 °C at 2000 ×*g* for 10 min with 30 s pauses, and the supernatant was removed. Then, 2D rehydration buffer was added to the samples (8 M urea, 2 M thiourea, 4 % CHAPS, 30 mM Tris pH 8.5, and protease inhibitor cocktail). Stainless steel beads of 0.2 mm size were used to lyse the samples, and the samples were homogenized by a Next Advance (USA) homogenizer. Then, they were centrifuged at 4 °C 15,000 ×*g* for 30 min 3 times. The solubilized protein-containing supernatants were transferred into fresh Eppendorf tubes. After that, by performing a Bradford assay (Bio-Rad, USA), protein concentrations were determined (Yanar et al., 2023) using a NanoDrop ND-1000 spectrophotometer (Thermo Scientific, USA), and the proteins were stored at −80 °C. The homogenous sample pool was prepared by mixing equal amounts of protein from each sample in a single tube, and the concentration was measured once more by Qubit Protein Assay (Thermo Fisher Scientific, USA) for further assays.

2.2.2. Liquid chromatography (LC) tandem MS/MS analysis and MS data analysis

Equal amounts of protein from each pooled sample were digested using an in-solution tryptic digestion and guanidination kit following the manufacturer's protocol (Thermo Fisher, MA, USA) for identification by nLC–MS/MS. Digested peptides were analyzed in duplicate by nLC–MS/MS using an Ultimate 3000 RSLC nanosystem (Dionex, Thermo Fisher Scientific, USA) coupled to a Q Exactive mass spectrometer (Thermo Fisher Scientific USA) with an electrospray ion source, and the system was controlled by Xcalibur 4.0 software as described by Akpinar et al. (2021).

Proteome Discoverer SEQUEST (version 2.2, Thermo Fisher Scientific, USA) software was used to analyze raw MS/MS fragmentation spectra and then searched against the UniProt/Swissprot *Danio rerio* reference proteome database with all isoforms (txid7955). To identify the proteins, the setting parameters were selected as explained by Albayrak et al. (2022). The filtered retrieval results by the software were as follows: if their probability was ≥95 and 99 % and consisted of two or more identified peptides, then the peptide and protein identifications were accepted. The false discovery rate (FDR) threshold was set to 0.01 (strict), and the target FDR (relaxed) was 0.05 using the Percolator node.

2.2.3. Bioinformatics analysis

Student's *t*-test was performed to determine the statistical significance (p value ≤ 0.05) of the protein quantitation data. Hierarchical clustering analysis and heatmap, principal component analysis (PCA) and PCA score plotting, and volcano plot analysis with graphics and significance of the protein quantitation were performed using GraphPad Prism 9.1.0 (La Jolla, CA, ABD) software. The functional enrichment analysis was performed as DEP classification based on gene ontology (GO) categories in an online database (http://www.geneontology.org) (Carbon et al., 2021). Fisher's exact test and Bonferroni correction for multiple testing were selected to adjust the derived p values, and $p < 0.05$ was considered significantly enriched. The GO terms grouped into ontologies as biological process (BP), cellular component (CC), and molecular function (MF). The gProfiler enrichment analysis (Raudvere et al., 2019) was performed online (https://biit.cs.ut.ee/gprofiler/gost) with the selected g:SCS threshold and $p < 0.05$ as the user threshold. Pathway enrichment analysis was performed based on KEGG, Reactome and Panther pathway enrichment analyses using KOBAS online tools (http://kobas.cbi.pku.edu.cn/)) (Bu et al., 2021) with a threshold of $p < 0.05$. The protein–protein interaction (PPI) network associated with molecular changes was constructed using the Search Tool for the Retrieval of Interacting Genes database (http://www.string-db.org) (STRING v11). The confidence score was selected as >0.9 and used as the cut-off criterion. The first and second shells were selected as five interactors.

2.3. Gene expression analysis-q-PCR assay

2.3.1. RNA isolation and q-PCR analysis

PCRs were performed with three biological pooled samples within each pool containing three zebrafish livers ($n = 9$) and two technical replicates (for the control and treated groups). Suitable primers were designed using the Thermo Fisher OligoPerfect Primer Designer (https://apps.thermofisher.com/apps/oligoperfect) application and analyzed with the IDT Oligo Analyzer (https://www.idtdna.com/calc/analyzer). The target genes were catalase (*cat*), glutathione peroxidase (*gpx*), acetylcholinesterase (*ache*) and pregnan x (*pxr*), while glyceraldehyde-3-phosphate dehydrogenase–GAPDH (*gapdh*) and actin (*β-actin*) were internal control housekeeping genes. The primers are listed in Supp. Table 6. The expression levels of the target and internal control genes were measured by quantitative real-time PCR. β-Mercaptoethanol (Merck, Germany) was prepared for the total RNA extraction of zebrafish liver tissues, and RNA isolation was performed using the PureLinkTM RNA Mini Kit (Thermo Fisher Scientific, Waltham, MA, USA) according to the manufacturer's protocol. The quality and quantity of isolated RNA were evaluated by calculating the OD260 nm/OD280 nm ratio on a Cytation 3 multimode reader. RNA sample values between 1.8 and 2.0 were accepted as suitable for further cDNA reverse transcription with a High-Capacity cDNA Reverse Transcription Kit (Thermo Fisher Scientific, Waltham, MA, USA) following the protocol. Quantitative real-time PCR using SYBR Green qPCR mix and qRT-PCR analyses were performed on a Roche LightCycler 96 (Roche-Switzerland) PCR detection system. In brief, after an initial step at 95 °C for 15 s, annealing at 60 °C for 15 s and extension at 72 °C for 1 min were performed. The amplifications were conducted with 40 cycles, and the annealing temperature (60 °C) was also set as the melting point for our primers. An amplification melting curve assay was performed between 60 °C and 95 °C with an increment of 0.15 °C/s to verify the reaction specificity. PCR efficiency calculated for all primers. The relative expression data were normalized to the geometric mean of the two housekeeping genes (*gapdh* and *β-actin*). The relative expression levels were calculated with the ΔΔCt method (Vandesompele et al., 2002; Hellemans et al., 2008). Both relative expression levels and fold change presented graphics performed by Graph Pad Prism software (v9, San Diego, CA, USA).

2.4. Biochemical analysis

2.4.1. Tissue homogenate preparation

Ten zebrafish (n = 10) each for the control and IMI-treated groups were sacrificed by applying hypothermia. To prepare homogenate, the liver tissues taken from the freezer were thawed on ice and transferred into sterile 2 mL tubes with 1:10 (w/v) cooled homogenate buffer consisting of sodium phosphate and sucrose. Then, samples were fragmented in a homogenizer with the help of glass beads. The amount of tissue diluted was determined in advance by preroutine trials. The samples were centrifuged at 10,000 ×*g* for 30 min at 4 °C. Then, with caution, the supernatant was transferred to new tubes, and the pellets were discarded. The biochemical analyses were performed manually following the steps of the protocols.

2.4.2. Oxidative stress-related biomarker assays

CAT is an antioxidant enzyme that catalyzes the transformation of hydrogen peroxide to water and is detected by a decrease in absorbance at 240 nm. The reduction in absorbance in 1 min is a marker of catalase activity (Aebi, 1984). The GSH assay was performed to determine the GSH content, formed by the reaction of DTNB and sulfhydryl groups' light absorption of the colored product at 412 nm determined spectrophotometrically and evaluated in nmol GSH/g protein (Beutler, 1975).

MDA content assessment was conducted based on the (Ledwożyw

et al., 1986) method where read at 532 nm. The data are expressed as nmol MDA/g protein. AChE enzyme activity measured by the (Ellman et al., 1961)method. AChE activity was assessed at a wavelength of 412 nm and calculated in U/mg protein. To determine the protein amount in the liver tissue of zebrafish (Bradford, 1976) at 595 nm 15 min after mixing with reagent, the counter absorbance was recorded, and the protein amount was expressed in μg/μL. The steps followed to calculate the statistics of the biochemical parameters as the data first checked for normality and distribution by calculating the Shapiro–Wilk test. Then, Student's *t*-test was used to determine the significance and a p value $<$ 0.05 was accepted as significant. The data analyzed are presented as the mean $\pm$ standard deviation (n $=$ 10). Data analyses and plots were generated with Graph Pad Prism software (v9, San Diego, CA, USA). The p values were shortened with the following symbols: $*p < 0.05$, $**p < 0.01$, $***p < 0.001$, $****p < 0.0001$ and ns: nonsignificant.

3. Results

3.1. Proteomic analysis

3.1.1. An overview of IMI exposure effects on the liver proteome

In this study, we identified a total of 958 quantifiable proteins in zebrafish liver tissue. The differentially expressed protein (DEP) threshold was set as $p \leq 0.05$. The DEPs above the threshold were grouped into two categories and named as if FC $\geq$ 2 upregulated if not downregulated. Due to the abovementioned criteria, a total of 86 (52 upregulated and 44 downregulated) differentially expressed proteins (DEPs) were identified and are listed in Table 1 with their accession number, regulation trend, FC, and p values. In addition, the DEPs of $p \leq$ 0.05 with ranging FC and short definitions are listed in Supplementary data Table 3. (It is crucial to state the MS data analyzer program is able to measure and report fold change of maximum1000 as the highest value both for up and down regulated proteins.) Among these significant 86 proteins, 20 (%23.26) were upregulated by 1000 FC, and 11 (%12.79) were downregulated by 1000 FC in the control group, as shown in Fig. 1A pie chart. In this paper, we refer to these extremely up- and downregulated DEPs as extremely upregulated (EU-DEPs) and extremely downregulated (ED-DEPs). In addition, we detected proteins that were not that extreme but still significant, with 32 % (37.21) upregulated (FC $\geq$ 2–50) and 23 % (26.74) downregulated (FC $\leq$ 0.5–0.01), as shown in Fig. 1A. Selected proteins included in EU-DEPs were lysozyme, sulfurtransferase, Aldh9a1b protein, hemoglobin, catenin, trypsin, glutaredoxin, and carboxypeptidase B1 proteins. The proteins involved in ED-DEPs were 60S ribosomal protein, Derlin, glutathione S-transferase and eukaryotic translation initiation factor. However, we underline the selected DEPs higher than the threshold with FCs of 50.35, 18.03, 10.67 and 9.97 for trypsin, glutaredoxin, Cyb5a protein and carboxypeptidase B1, respectively. In addition, we detected eukaryotic translation initiation factor-3, oxysterol-binding protein and epimin with an FC of 0.001 as downregulated DEPs. The regulation

Table 1
Regulation trends of 86 differentially expressed proteins (DEPs) ($p \leq 0.05$) with their accession numbers, fold changes, and actual p-values are listed.

Regulation	Accession no	Fold change	p-Value	Regulation	Accession no	Fold change	p-Value
UP	A0A2R8RWI8	1000	3.1E−16	*UP*	Q5TYY5	3.4	2.7E−02
UP	Q32PK8	1000	3.1E−16	*UP*	A0A0G2KZR6	3.3	3.3E−02
UP	F1R8J6	1000	3.1E−16	*UP*	Q6P5J0	3.2	3.9E−02
UP	E7FCV8	1000	3.1E−16	*UP*	A0A0R4IM99	3.2	3.9E−02
UP	F1QVX3	1000	3.1E−16	*UP*	A1L259	3.2	4.0E−02
UP	A0A1D5NSP9	1000	3.1E−16	*UP*	Q6PHD8	3.2	4.1E−02
UP	A0A2R8RQT4	1000	3.1E−16	*UP*	Q6DH80	3.2	4.1E−02
UP	F1QLV5	1000	3.1E−16	*UP*	F1QCN0	3.2	4.2E−02
UP	A0A2R8Q9V1	1000	3.1E−16	*UP*	Q6PFT7	3.1	5.3E−02
UP	F1Q9R5	1000	3.1E−16	*DOWN*	Q6P6E7	0.4	4.8E−02
UP	F1R9R1	1000	3.1E−16	*DOWN*	Q7ZUR5	0.4	4.5E−02
UP	Q6AZC0	1000	3.1E−16	*DOWN*	Q7T390	0.4	4.2E−02
UP	A0A2R8QRM9	1000	3.1E−16	*DOWN*	Q8AW82	0.4	4.2E−02
UP	A0A2R8PVJ3	1000	3.1E−16	*DOWN*	F2WZ27	0.4	4.1E−02
UP	Q4V8Q9	1000	3.1E−16	*DOWN*	F1R5R0	0.4	4.1E−02
UP	Q0P4B4	1000	3.1E−16	*DOWN*	Q7ZVS4	0.4	4.1E−02
UP	B2GT49	1000	3.1E−16	*DOWN*	Q5TZG1	0.4	3.9E−02
UP	Q6ZM13	1000	3.1E−16	*DOWN*	A0A2R8QAA9	0.4	2.5E−02
UP	A9JRW0	1000	3.1E−16	*DOWN*	E7F427	0.3	1.2E−02
UP	F1QWD0	1000	3.1E−16	*DOWN*	Q7ZWB4	0.3	1.0E−02
UP	Q9DDE1	50.4	3.1E−16	*DOWN*	F1Q8C3	0.3	6.8E−03
UP	F1QLM7	18.0	3.6E−13	*DOWN*	Q08BF2	0.3	5.1E−03
UP	Q6IMW7	11.7	1.9E−09	*DOWN*	F1QMB0	0.2	2.9E−04
UP	A8WGS0	10.7	9.8E−09	*DOWN*	Q6DHB9	0.2	2.3E−04
UP	F1QJN9	10.0	3.1E−08	*DOWN*	Q6IMW8	0.2	1.0E−04
UP	Q1LYB7	8.6	3.7E−07	*DOWN*	Q5BLE6	0.2	2.8E−05
UP	Q7ZVA4	8.1	8.9E−07	*DOWN*	A0A0R4J8E6	0.2	2.1E−05
UP	Q7ZU89	7.8	1.7E−06	*DOWN*	A0A0R4IXF5	0.2	1.1E−05
UP	F1QUN8	7.6	2.3E−06	*DOWN*	Q7SXI0	0.2	1.1E−05
UP	Q7ZZA3	7.6	2.3E−06	*DOWN*	B5DDP0	0.1	2.2E−08
UP	Q6PH72	6.5	1.9E−05	*DOWN*	A0A0N4SU47	0.1	4.7E−09
UP	Q66I77	6.2	3.6E−05	*DOWN*	Q6IQR6	0.011	3.1E−16
UP	Q5RKM9	5.9	7.2E−05	*DOWN*	Q6DI12	0.001	3.1E−16
UP	F8W4J1	5.8	8.7E−05	*DOWN*	F1R8Q3	0.001	3.1E−16
UP	A0A2R8RJY4	5.0	5.5E−04	*DOWN*	Q6DGM0	0.001	3.1E−16
UP	B3DFS9	4.8	8.4E−04	*DOWN*	F1Q4W3	0.001	3.1E−16
UP	Q6PHI8	4.6	1.5E−03	*DOWN*	A0A2R8QDF0	0.001	3.1E−16
UP	E9QDI1	4.3	3.0E−03	*DOWN*	Q7SXZ5	0.001	3.1E−16
UP	Q4VBT8	4.2	3.3E−03	*DOWN*	F1QQW9	0.001	3.1E−16
UP	A5PF59	4.2	3.8E−03	*DOWN*	P17561	0.001	3.1E−16
UP	B8A5M6	4.2	3.8E−03	*DOWN*	A0A0R4ISN6	0.001	3.1E−16
UP	Q503E6	3.8	8.9E−03	*DOWN*	F6P8R2	0.001	3.1E−16
UP	F8W3C3	3.7	1.1E−02	*DOWN*	Q7T2A5	0.001	3.1E−16

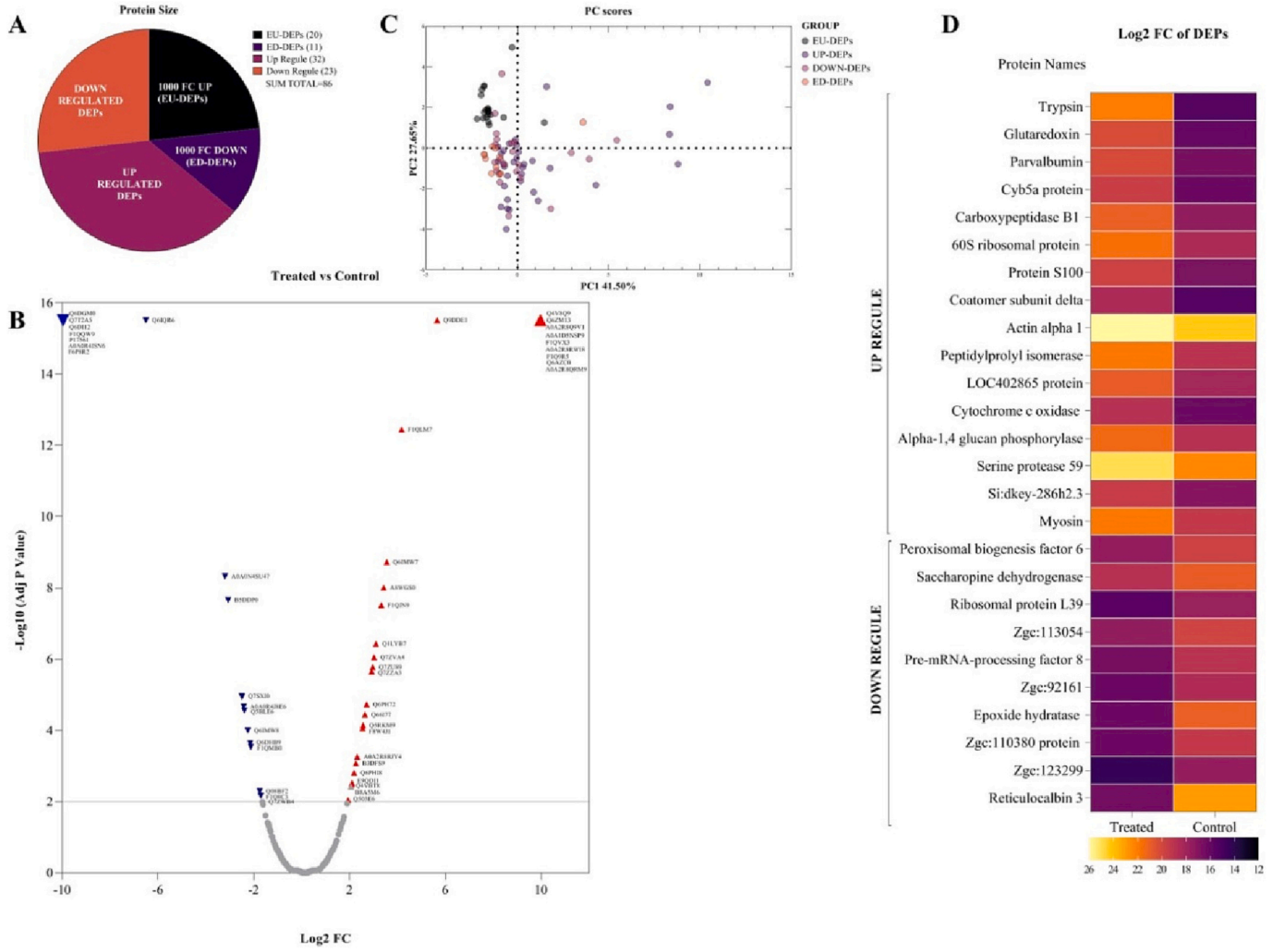


Fig. 1. An overview of IMI exposure effects on the zebrafish liver proteome is shown. A - Pie chart shows the distribution of 86 DEPs in the liver proteome ($p \leq 0.05$). B - Volcano plot shows 957 identified proteins. A threshold of log10 $p > 2$ (corresponding to adjusted $p < 0.01$) and log2 FC > 2 was set. Protein values above the threshold were considered to be differentially expressed. Non-DEPs are represented by gray dots, while Down-DEPs and Up-DEPs are represented by blue and red triangles, respectively. The EU-DEPs and ED-DEPs are represented by bigger red and blue triangles, respectively. C - Principal component analysis (PCA) was performed on the proteins that met the criteria of $p \leq 0.05$ and FC < 0.05–FC > 2, which included both EU-DEPs and ED-DEPs. The score graphic shows the variance of four primary groups of DEPs ($p \leq 0.05$). D - Heatmap of 26 DEPs ($p \leq 0.0001$), excluding EU-DEPs and ED-DEPs, shows a similar relationship among the samples and a tendency for upregulated expression from control to treated groups.

trends of the 86 DEPs with $p \leq 0.05$ are shown in Table 1, and the proteins involved in EU and ED-DEPs are listed with their brief definition in Supp. Table 1.

PCA was performed to evaluate the quantitative repeatability, as the two-dimensional scatter plot indicated considerable repeatability (Fig. 1C). The cumulative proportion of variances was 27.65 % for PCA1 and 41.50 % for PCA 2. PCA intended to spot the largest origin of variation in the data that is not based on groups. The absence of a remarkable difference between them does not indicate the absence of significant variation (Valdés et al., 2021). In addition, the volcano plot in Fig. 1C shows an overview of the differential expression of all proteins identified. The heatmap based on the expression patterns of 26 DEPs demonstrated a similar relationship among the samples and a tendency for upregulated expression from the control to treated groups (Fig. 1D).

3.1.2. Functional enrichment analysis of DEPs

We performed GO analysis via the gProfiler enrichment web service to classify clusters of BP, MF, and CC. As shown in Fig. 2A, GO (BP) terms of upregulated DEPs (EU-DEPs and upregulated DEPs together) were mapped as relevant to ROS (reactive oxygen species) metabolic process and response to xenobiotic stimulus. In terms of MF, catalytic and antioxidant activities and binding function were significant. For the CC classification, the most significantly mapped enrichment terms were cytoplasm and intracellular anatomical structure. Additionally, as shown in Fig. 2B, GO (BP) terms of downregulated proteins (ED-DEPs and downregulated DEPs together) were mapped as relevant to metabolic processes (e.g., lipid, monocarboxylic acid, oxoacid), but only 8 % of them were mapped as related to lipid biosynthetic processes. Additionally, catalytic activity with 90 % enrichment percent dominated the (MF) enrichment analysis with the mapped terms oxidoreductase and activities.

3.1.3. Pathway enrichment analysis of DEPs

The pathway enrichment analysis was performed following the functional enrichment analysis, while significant protein functions were expected to be reflected by the pathway enrichment. To analyze 86 DEPs in detail, they were grouped into two groups: upregulated and downregulated. Afterward, they mapped separately on the KOBAS online web service to generate KEGG, Reactome, and Panther pathways, as shown in Fig. 3. The enrichment results (p values and ratios) of the up- and

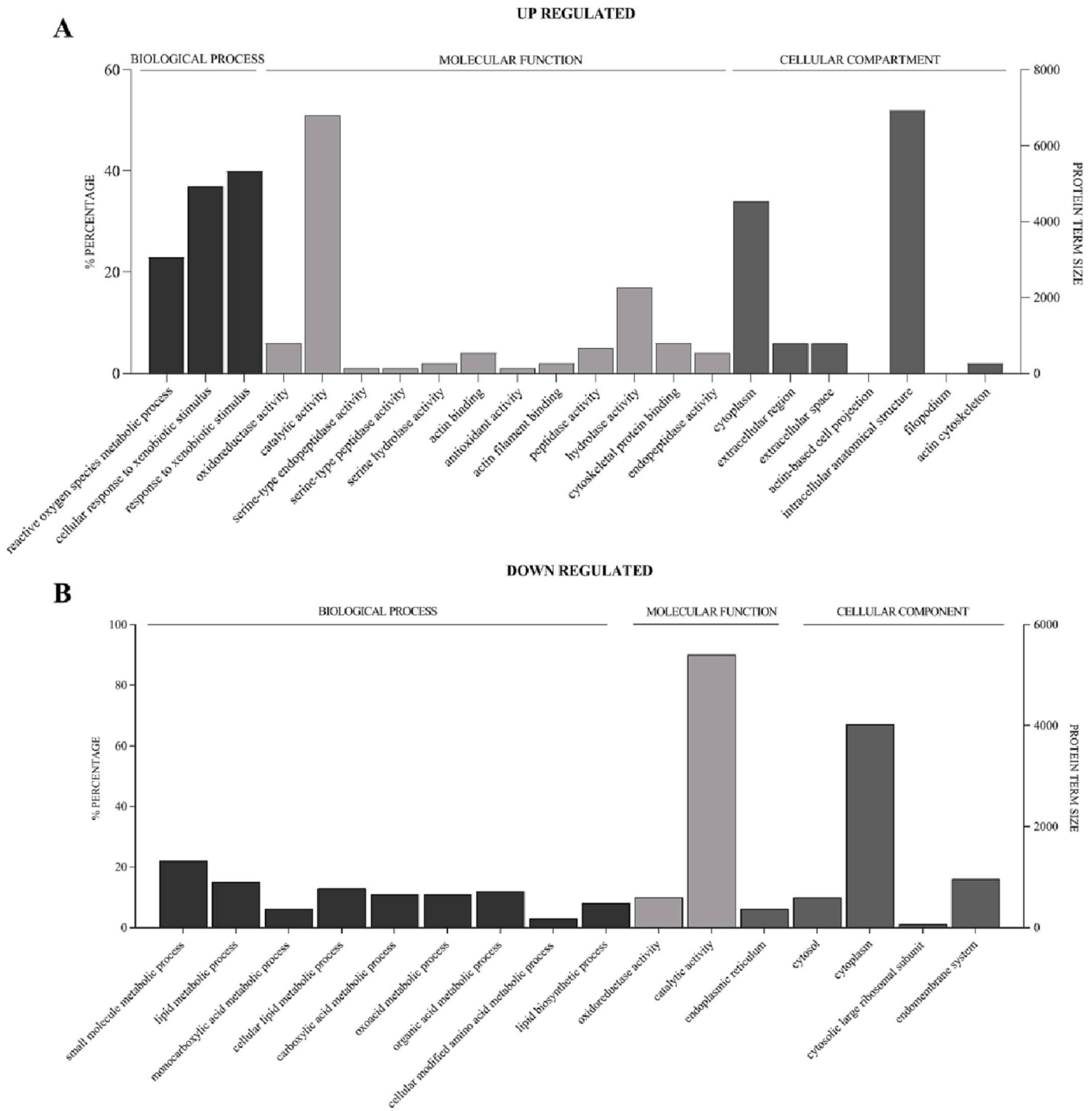


Fig. 2. Enrichment analysis was performed using gProfiler enrichment web service based on gene ontology (GO) terms. The analysis grouped the terms into biological process (BP), cellular component (CC), and molecular function (MF) ($p \leq 0.05$). The gProfiler enrichment analysis options were selected *Danio rerio*, all results, all known genes, g:SCS threshold, 0.05 as user threshold, and enterezgene_acc as numeric IDs treated. The enrichment analysis results for the A - Up-DEPs and B - Down-DEPs are shown. The size of protein terms is presented as a percentage on the left-hand side and as size at the right-hand side.

downregulated pathways are listed in Supp. Tables 3 and 4. The upregulated pathways were mainly related to sulfur metabolism (*sulfur relay system*), cellular metabolism (*ubiquinone and other terpenoid-quinone biosynthesis*), cellular catabolic process (*other glycan degradation*), and antioxidant activity (*ascorbate and aldarate metabolism*), as shown in Fig. 3A. The other upregulated pathways were involved in amino acid metabolic *processes* (*histidine metabolism and function*), cell–cell *junctions* (*tight junctions*), oxidative metabolism (*beta-alanine metabolism*), and cell–cell signaling pathways (*Wnt signaling pathway*).

As shown in Fig. 3B. The downregulated pathways were involved in gene expression (*protein processing in endoplasmic reticulum and cap-dependent translation initiation*), transporter activity (*one carbon pool by folate and primary bile acid biosynthesis*), oxidoreductase activity (*butanoate metabolism*) and cellular processes (*biosynthesis of unsaturated fatty acids, fatty acid elongation, GABA synthesis and ABC-family protein-mediated transport*). Moreover, they were involved in the metabolism of xenobiotics by the cytochrome P450 pathway, as shown in Fig. 3B.

3.1.4. Protein–protein interaction analysis of DEPs

STRING software was used to map and analyze the protein–protein

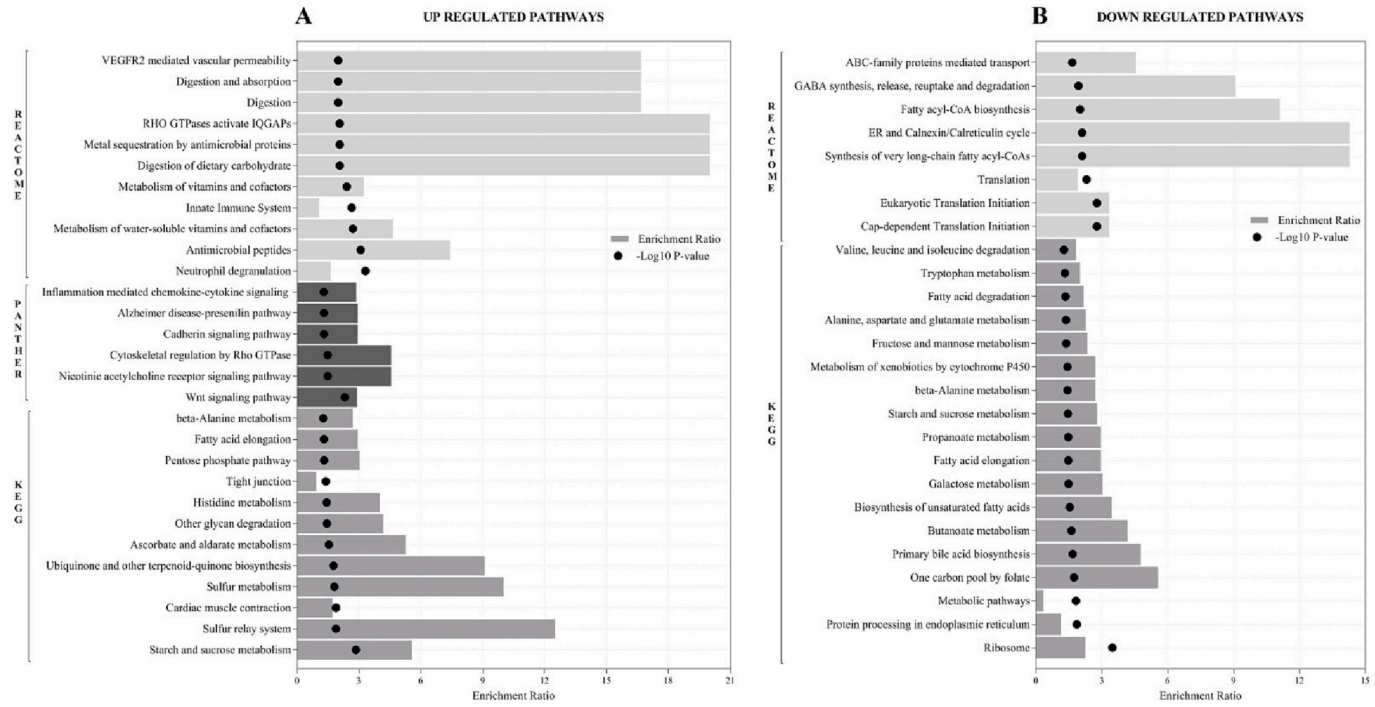


Fig. 3. KOBAS pathway enrichment analysis results show KEGG, Reactome, and Panther pathway terms ($p \leq 0.05$) of A - upregulated and B - downregulated pathways. The results show in bar plots of enrichment ratios and dot plots of the negative log10 *p*-values. The analysis threshold was $p < 0.05$ for the species *Danio rerio*.

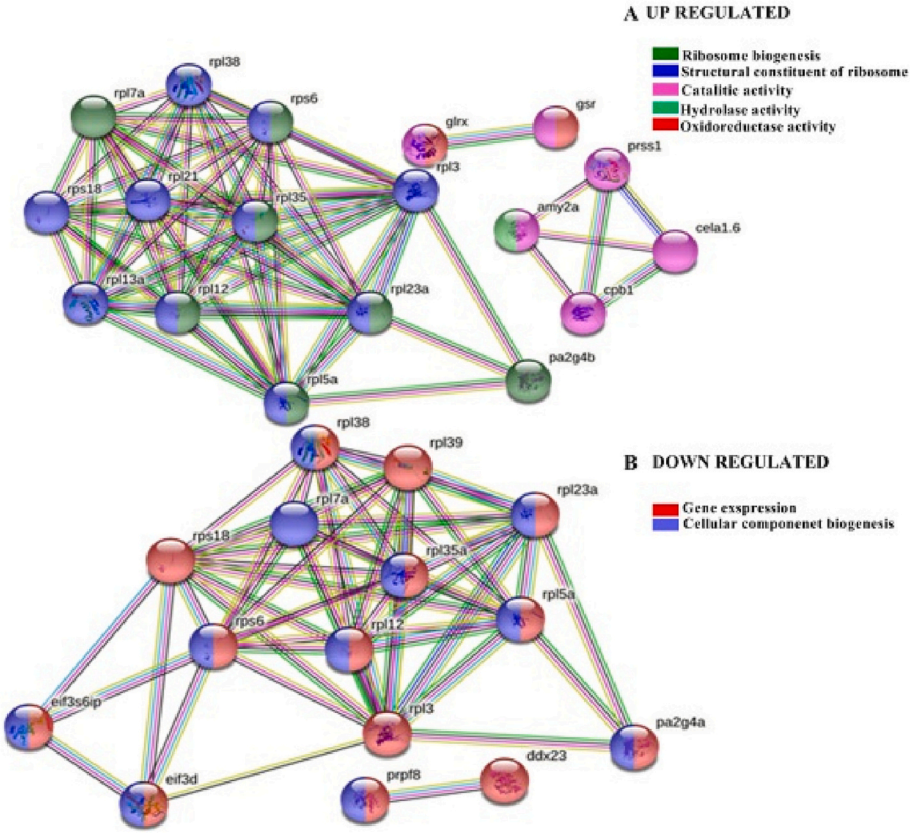


Fig. 4. Protein-protein interactions (PPI) of 86 DEPs were mapped and analyzed using STRING software. The EU-DEPs and Up-DEPs were merged into an upregulated group, while the ED-DEPs and Down-DEPs were merged into a downregulated group. Both groups were analyzed separately to create PPI and shown as A - upregulated and B - downregulated.

interactions of 86 DEPs. To simplify the interpretation and presentation, the EU-DEPs and Up-DEPs were combined into one group, and the same process was performed for ED-DEPs and Down-DEPs. Then, they were separately analyzed for PPI analysis as up- and downregulated, as presented in Fig. 4A–B. The upregulated protein interactions were mainly between ribosome biogenesis and the structural constituents of ribosomes, as shown in Fig. 4A. Moreover, the upregulated proteins involved in catalytic, hydrolase, and oxidoreductase activities were mapped and are shown in Fig. 4A. The downregulated protein interactions were mainly between the proteins involved in gene expression and cellular component biogenesis, as presented in Fig. 4B.

3.2. Effects of IMI on the expression levels of the selected genes

The expression profiles and fold changes of the *cat*, *ache*, *gpxr* and pxr genes are shown in Fig. 5. The statistically downregulated genes were the *cat* and *gpxr* genes compared to the control ($p < 0.005$), and the *pxr* gene was insignificantly downregulated, whereas the *ache* gene was significantly upregulated ($p < 0.0005$). The regulatory pattern is presented as the log2-fold change in Fig. 5.

3.3. Effects of IMI on the selected biochemical parameters

As shown in Fig. 6, CAT ($p < 0.0005$) and AChE ($p < 0.05$) enzyme activities significantly increased compared to the control. The GSH content also significantly increased ($p < 0.05$). Furthermore, the MDA level and total protein amount significantly decreased ($p < 0.05$).

In this study, after we grouped the results according to the cutoff criteria, we analyzed the proteomic outcomes via bioinformatics online applications. Bioinformatics analyses are mainly based on the enrichment of proteins and pathways. Furthermore, we tested the statistical significance of the gene expression and biochemical parameter results.

4. Discussion

Widely used IMI residuals (Morrissey et al., 2015; Thunnissen et al., 2020) that possibly cause various adverse effects on nontarget aquatic organisms were found in water bodies. Consequently, these studies shed light on other researchers; Luo et al. (2021c) reported the effect of IMI on zebrafish gut and intestine exposed to 100 and 1000 μg/L IMI for 21 days, and Thunnissen et al. (2020) reported the ecological risks of IMI to aquatic species at the assessed concentrations (Thunnissen et al., 2020). Among several studies performed with the biochemical and gene expression approaches concurrently on zebrafish examining IMI effects (Shukla et al., 2017b; Sposito et al., 2018; Guerra et al., 2021; Queiroz et al., 2021; Zhang et al., 2021; Luo et al., 2021b), we chose (Reinwald et al., 2022) because it was unique in that it studied with an omic; transcriptomic approach analyzing the adverse effects of five pesticides (one of them was IMI) on (even though) zebrafish embryos exposed to 15, 30 and 60 mg/L IMI for 96 h duration. According to data mining studies, there seems to be a requirement for complementary analyses of multiapproach studies on the effects of IMI on zebrafish liver. We chose a multiapproach study design to comprehend to what extent IMI affected zebrafish liver in the context of the proteome, with the selected transcript and activity levels of the oxidative stress response components. Therefore, we carried out a multiapproach experimental design comprising proteomics molecular and biochemical analyses.

4.1. Evaluation of IMI effects by the proteomic approach

To interpret the proteomic approach outcomes of the liver exposed to IMI, we analyzed the crucial functions of the proteome. The mapped upregulated protein terms were linear with our expectations, such as ROS metabolic process, cellular response to a xenobiotic, and response to xenobiotic stimulus, which were considerably upregulated. In line with these outcomes, we found that catalytic activity (Fig. 3) notably upregulated with other molecular defense systems, such as oxidoreductase, antioxidant, and hydrolase activities (Lin et al., 2018; Tierbach et al., 2018; Araújo et al., 2022; Gao et al., 2022; Kwon et al., 2022; Reinwald et al., 2022). The downregulated proteins in this study were involved in lipid and organic acid metabolic processes with notably high catalytic and oxidoreductase activities. Similarly, Lin et al. (2018) detected downregulated proteins related to microtubule-based processes, protein polymerization, and oxygen transport.

The second parameter to interpret the proteomic approach outcomes of the liver exposed to IMI was the prominent pathways of the liver proteome. The upregulated proteins mapped to pathways specifically linked with catalytic, transporter, antioxidant metabolism, cellular process, molecular function regulator, binding, cellular processes, immune system, antimicrobial activity, energy metabolism, and cell communication biological functions (Fig. 3); we interpreted this as a marginal response that emerged as upregulation of stress-related pathways, and initiation of these pathways altogether eventually caused significant damage. Based on these findings, we underlined that IMI has disruptive effects on the functioning of many systems, at most defense, energy metabolism and neuro-protective systems of the organism. In line with our study, Piña et al. (2019) investigated the effects of an acetylcholinesterase inhibitor used as a pesticide and showed upregulated stress-associated pathways with downregulated proteins related to the nervous system. A similar study with zebrafish liver exposed to the pesticide dieldrin reported its response as altered pathways related to centrosome separation, glucose/energy metabolism, and the immune system (Simmons et al., 2019).

The downregulated enriched pathways were related to gene expression, neuroprotective and antioxidant activities, response to stress, and folding quality control. While the mode of action of IMI is acting as a nicotinic acetylcholine receptor (nAChR) agonist in the central nervous system (Luo et al., 2021a), the downregulation of the

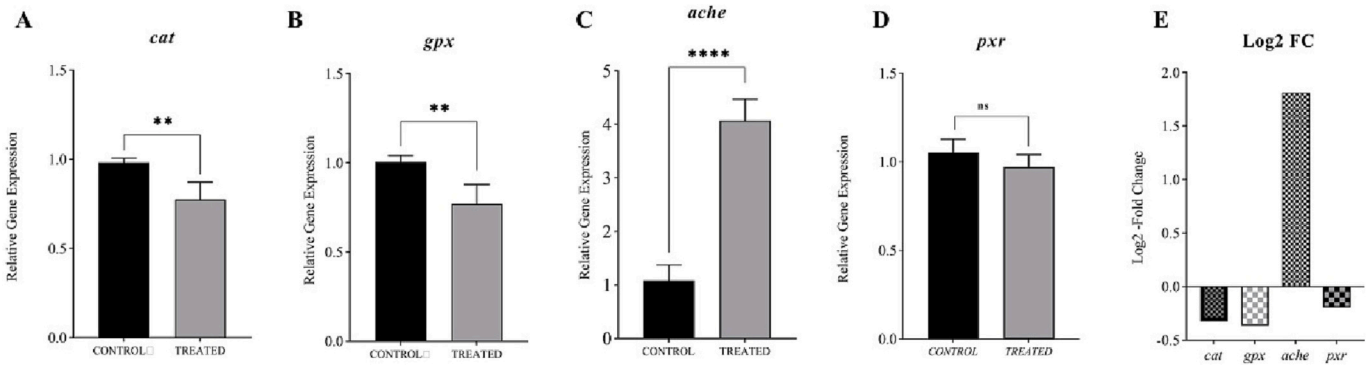


Fig. 5. Oxidative stress-related genes were selected as *cat*, *ache*, *gsh*, *pxr*. Bar plots show the relative gene expression profiles and log2 fold changes of the selected genes, respectively A, B, C, D, and E (*$p < 0.05$, **$p < 0.005$, ***$p < 0.0005$ and *ns*: nonsignificant).

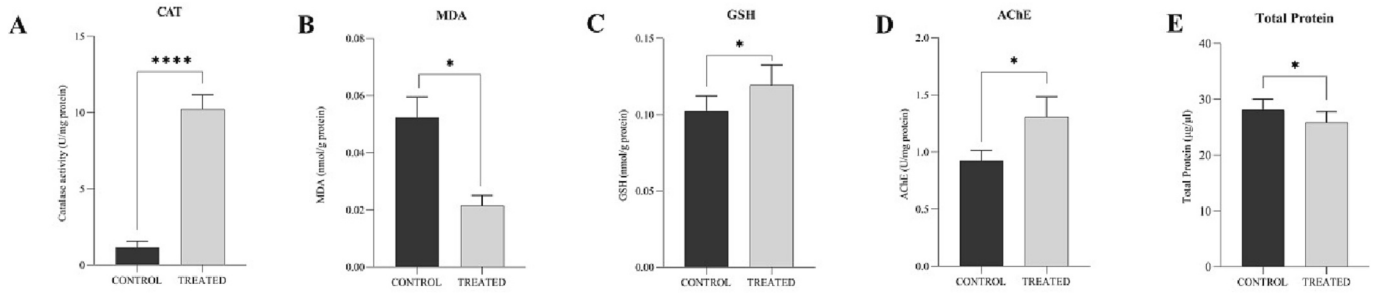


Fig. 6. Biochemical oxidative stress-related parameters were selected: CAT enzyme activity, MDA level, GSH content, AChE enzyme activity, and protein amount. Bar plots show the parameters of A - CAT enzyme activity, B - MDA level, C - GSH content, D-AChE enzyme activity, D - Protein amount (*$p < 0.05$, ****$p < 0.00005$ and *ns*: *nonsignificant*).

neuroprotective pathway was expected. Thus, we emphasize the neurodegenerative effect, yet further studies should be performed on the zebrafish brain. On the other hand, we observed both upregulation of the antioxidant metabolism pathway and downregulation of the xenobiotic stimulus response, which seemed contradictory at first, but we considered this result to be an indicator of the maximum stress level reached.

Second, we emphasize the adverse effects of IMI on protein quality-related endoplasmic reticulum (ER) stress. We determined that the stress resulting from exposure to IMI is high enough to stimulate crucial defense systems of the organism. Hence, we observed that lipid process and folding quality pathways were downregulated, as these pathways are controlled by the ER (Gao et al., 2022). Stress conditions affect the ER and its functions and thus result in protein import exceeding the protein folding capacity, which initiates the unfolded protein response (Kaokhum et al., 2022). Consequently, the inability to overcome ER stress gives rise to cellular dysfunction, cell death, apoptosis, and diseases such as neurodegeneration and cancer (Kaokhum et al., 2022), suppressing almost all defense mechanisms of organisms, thus being in danger of significant disorders (Horzmann et al., 2018; Sürmen et al., 2021) and survival (Vieira et al., 2020). In short, with this study, it has been determined that the stress resulting from exposure to IMI is high enough to stimulate crucial defense systems of the organism.

In our study, we identified several unanticipated proteins involved in the two marginal groups named EU-DEPs and ED-DEPs (Supp. Table 1). As a necessary step to clarify selected proteins involved in EU-DEPs, we first observed thiosulfate sulfurtransferase (TST) due to its importance in sulfide (H2S) metabolism and the degradation of ROS. Accordingly, our study was in line with (Al-Dahmani et al., 2022), who reported that excessive amounts of dissolved thiosulfate in tissue lead to the blocking of mitochondrial cytochrome complex IV, hence causing sulfide-induced oxidative stress. Therefore, we can underline its importance as an IMI adverse effect primarily as oxidative stress.

Palmitoylation, the EU-DEPs (Supp. Table 1), is the posttranslational addition of a fatty acid chain to proteins that affects protein stability and function, membrane transport, and subcellular localization, while PPT1 depalmitoylation activity is considered necessary for protein degradation (Xie et al., 2022). The palmitoylation/depalmitoylation reaction regulates subcellular localization, and its disrupted regulation could lead to neurodegenerative disorders (Hong et al., 2020). Palmitoylation of the transistent receptor in neuronal-striatal cells was shown by Hong et al. (2020) and stated as a response to abnormal oxidative stress that ROS could cause cell death. Although, in this study, we performed on the liver, not the brain, we interpret the observed high palmitoyl-protein thioesterase expression as a response of cells to neonicotinoid insecticide and possibly an indicator of oxidative stress-related neurodegenerative disorder.

ROS production is accepted to be related to the Wnt/β-catenin signaling pathway and is known for its vital role in regulating cardiovascular development (Li et al., 2020, 2021). However, we observed both upregulation of oxidative stress-related proteins and extreme upregulation (EU) of the catenin protein (Supp. Table 1). However, contrary to our results, Huang et al. (2020) stated that upon exposure to the herbicide, zebrafish embryos responded by inhibiting the Wnt signaling pathway and downregulating its target gene (b-catenin). This contrast may arise from the developmental level of the organism (Glaberman et al., 2017) or the difference in pesticide modes of action. As a crucial role, the Wnt/β-catenin signaling pathway protects tissues and organs from oxidative stress-induced apoptosis (Zancan et al., 2015; Huang et al., 2020). Thus, the extreme upregulation of catenin protein was considered, as it could probably initiate oxidative stress in conjunction with apoptosis protective mechanisms.

Clarifying the selected proteins involved in ED-DEPs is also a necessity (Supp. Table 2). The first protein in this group was folate, which is essential for nucleic acid and protein synthesis with DNA repair and methylation pathways. Folate deficiency was observed to induce oxidative stress (Chen et al., 2018). We measured ED-regulated cytoplasmic C1 tetrahydrofolate (C1-THF) synthase, which inhibits its role in repairing oxidative DNA damage, and concluded that IMI exposure could both induce oxidative stress and lead to diseases due to unrepaired DNA damage.

Derlin included in ED-DEPs (Supp. Table 2) is the key player in endoplasmic reticulum (ER) protein quality control, while ER stress reduction is pivotal since if not, cells initiate multiple apoptotic pathways that lead to cell death (Li et al., 2019). In our analysis, we tracked (ED)-regulated derlin1 protein levels in line with (Li et al., 2019), who also found that knockdown of derlin1 inhibited the cell proliferation and migration that contributed to apoptosis in cancer. Hence, we state that extreme downregulation of derlin1 inhibits ER stress control mechanisms and possibly initiates apoptosis in cells, resulting in diseases such as cancer and neurodegenerative disorders (Kandel and Neal, 2020). However, further specific analyses were mandatory to be sure whether apoptosis was triggered.

The oxysterol-binding protein (OSBP) family is a sensor and transporter of sterol that regulates lipid/cholesterol metabolism and steroid hormone synthesis (Wang et al., 2019), and one of its members is Oxysterol-binding protein like-2. We observed ED regulation of oxysterol-binding proteins (Supp. Table 2), and parallel with (Wang et al., 2019) conducted their experiment on Osbpl2 knock-out cells and assessed that reduction of this protein was associated with significantly increased ROS levels followed by mitochondrial damage. In addition, a lack of oxysterol-binding protein causes increased cholesterol biosynthesis by suppressing the AMPK signaling pathway, known as the energy sensor, which is responsible for sustaining energy homeostasis by coordinating efficacious metabolic responses to reduced energy availability (Collodet et al., 2019). With this result, we consider that IMI exposure prevented the stimulation of metabolic reprogramming and adjustments in the prolonged regulation of specific transcription factors and coactivators by suppressing the AMPK signaling pathway, therefore causing distortions in energy metabolism and presumably endangering

the survival of the organism in the long term.

4.2. Evaluation of IMI effects by oxidative stress-related biomarker analyses

In this study, we detected that the *cat* gene was downregulated, inconsistent with the elevated CAT enzyme activity. In line with our findings, Ni et al. (2019) observed downregulated *cat* gene expression and increased CAT enzyme activity in their study of antibiotic-exposed zebrafish. A similar study of zebrafish exposed to IMI (Luo et al., 2021c) reported downregulated *cat* gene expression levels and elevated CAT enzyme activity, in line with our measurements. In contrast to our downregulated *gpx* gene expression level and elevated GSH level, they detected decreased GSH content and *gpx* gene expression levels. Hence, we assume that this difference is due to the different exposure amounts and/or exposure durations. The discrepancies between the expression levels of genes encoding antioxidant enzymes and their activities could be because of the multiple gene clusters encoding an enzyme, the presence of multiple gene copies, the time delay impact between transcription and translation, and/or posttranslational modifications (Chen et al., 2017; Ni et al., 2019). Taken together, we derive that increased CAT activity and GSH content could be the guarding and flexible reply to oxidative stress induced by the studied pesticide (Chen et al., 2017).

The pregnane X receptor (PXR; NR1I2) regulates CYP3A4 expression and functions in the biotransformation of endogenous substances and drugs, consequently initiating the transcription of other genes involved in the metabolism, transport, and elimination of xenobiotics (Bresolin et al., 2005). The latest reports indicated its participation in the regulation of P450 genes and elicited crosstalk between zebrafish aryl hydrocarbon receptor (AhR) and PXR, thus suggesting a role in the detoxification of xenobiotics (Creusot et al., 2021). In this study, we observed nonsignificant upregulation of *pxr* gene expression. Similar results were observed by Bresolin et al. (2005) zebrafish exposed to a synthetic steroid and antianginal, resulting in insignificant upregulation of the *pxr* gene. Therefore, we suggest that the increase in the expression of the *pxr* gene level was an indicator of a triggered antioxidant system. Since these results were similar to other antioxidant markers, we concluded that the *pxr* gene is suitable to be evaluated as a marker in environmental toxicology studies.

During an attack of ROS on macromolecules, lipid peroxidation (LPO) occurs to form lipid peroxides, such as malondialdehyde (MDA), which affects the permeability and fluidity of the cell membrane, thus causing changes in cell structure and function (Jiao et al., 2020). To determine the degree of LPO as an indicator of oxidative stress, MDA is frequently used in toxicology studies (Ni et al., 2019; Kayhan et al., 2020). In this study, we observed a statistically significant decrease in MDA levels. Likewise, a low dose of herbicide affected zebrafish liver and decreased MDA content, as reported by Esmer Duruel and Kayhan (2021). Nevertheless, Luo et al. (2021a) measured the effects of IMI by applying different doses and detected an insignificant uptrend of MDA levels with significant elevation of CAT activity (only for high dose exposure group) along with unchanged GSH levels. Unlike our study, they observed consistency between cat enzyme and CAT activity. The reasons for the discrepancy between their and our results may be the tissue chosen, the duration of pesticide exposure, and the differences in pesticide doses applied. However, decreased MDA levels with increased CAT and GSH levels (as we observed) may induce apoptosis through endogenous antioxidant depletion and lipid peroxidation accumulation (Dong et al., 2018). In addition, increased CAT activity (as in our study) could probably scavenge H_2O_2, prevent cell membrane peroxidation of unsaturated fatty acids, and assist in reducing MDA content.

Acetylcholinesterase (AChE) activity alterations are accepted as a vital biomarker of neurotoxicity; therefore, AChE enzyme activity assays are frequently performed in ecotoxicology studies. In the present study, we observed upregulation of ache gene expression, which was consistent with the elevation of AChE enzyme activity. However, the effects of IMI on the brain tissue of rainbow trout were assessed by Topal et al. (2017b), similarly observed an increase in CAT activity but a decrease in AChE activity. The difference could be due to the selection of different species and/or the duration and quantity of the pesticide applied. A similar finding from Zhang et al. (2021) highlighted the increased activity of AChE and interpreted this as a potential neurotoxicity in larval zebrafish exposed to IMI. Although the AChE enzyme is acknowledged as a target of neonicotinoid insecticides in the brain and muscle tissues (Benli and Çelik, 2021), the results of this study contribute to the literature with its data that liver tissue may also be the target of IMI. Moreover, increased AChE activity is considered a marker and regulator of apoptosis, while its pharmacologic inhibitors prevent apoptosis (Benli and Çelik, 2021). Evaluated in conjunction, the present study propounded that IMI has a toxic effect on zebrafish that could probably lead to apoptosis and physiological impairments in many functions (Zhang et al., 2021).

4.3. Evaluation of IMI effects by complementary analyses of multiple approaches

In the current study, we carried out a complementary analysis to fill in the knowledge gaps on the adverse effects of IMI on the zebrafish liver model organism. In addition, this is the first study to evaluate IMI effects via a proteomic approach. Thus, proteins are the most prominent in vivo targets of oxidants in oxidatively stressed cells (Truong and Carroll, 2013). However, enzymatic activity alterations reflect the response of organisms to interventions at the biochemical level and ensure timely precaution for xenobiotic stress (Wu et al., 2018b). However, proteomics can provide information on the mechanisms of toxicity at low levels of organization (Reinwald et al., 2022) and is discerned as being "closer to phenotype", thus mirroring the exact activity in the cells and ensuring direct links to the processes and defense mechanisms regulated (Groh and Suter, 2015b). Based on the features above, the effects of IMI were studied using proteomics, biochemical, and molecular approaches, while it was estimated that a multiapproach would complement and reveal detailed elicit crucial outcomes.

Concise sums up of the proteomic results mainly highlighted the upregulation of xenobiotics and stress responses, antioxidant and binding activities, cell communication, and the immune response. In addition, upregulated ache gene expression with increased CAT and AChE enzyme activities and GSH content were highlighted. The upregulated enrichment analysis results were consistent with the oxidative stress parameter outcomes. The most prominent ones were triggered oxidative stress and antioxidant systems. The observed increased CAT enzyme activity and GSH content results were in accordance with the proteomic outcomes. Additionally, AChE enzyme and gene alterations highlighted possible adverse effects, such as neurodegenerative disorder, while elevated AChE enzyme activity is one of the indicators of neurodegenerative disorder. Although we observed the effects of IMI on the liver tissue but not the brain, future studies should focus on brain tissue to be sure about the impact of neurodegenerative adverse effects. In addition, critical consequences of oxidative stress-induced apoptosis have emerged, but this result also needs to be confirmed by other assays specific for apoptosis.

We observed downregulation of lipid metabolic processes, catalytic and oxidoreductase activities, gene expression, transporter activities, ER stress translation and signaling, neurological disorders, and *cat*, *gpx*, and *pxr* gene expression levels with decreased MDA levels. The up- and downregulated enrichment results complemented each other. For instance, the results of both downregulated xenobiotic stimulus response and upregulated antioxidative parameters were in line and indicated that the organism hit the maximum stress level that was also in line with the biochemical outcomes. However, among the downregulated proteome, the most noticeable results were related to the regulation of protein folding and transporting pathways since altered protein quality controlling mechanisms would ultimately and possibly

lead to the initiation of apoptosis and neurodegenerative disorders. Furthermore, in this study, we observed disrupted energy metabolism that eventually possibly inhibits energy homeostasis.

Our second and third approaches were molecular and biochemical markers evaluated together because the two methods were more likely to complement each other. However, our results were inconsistent CAT-*cat* and GSH-*gpxr* antioxidative stress gene enzyme association. The reasons for the inconsistencies between the mRNA and protein levels could be due to the following: 1 - very varied levels of mRNA and protein synthesis degradation, 2 - proteins have half-lives that range by orders of magnitude and are thus usually longer lived, 3 - their expression levels can quickly alter during responses to stress, and 4 - the vast majority of genes have early expression characteristics and are therefore expressed at the onset of exposure (Groh and Suter, 2015b).

Overall, we are aware of the rising challenges of applying omics approaches in ecotoxicological research, such as reproducibility, due to the lack of standardized analysis (Reinwald et al., 2022). Likewise, the vast amount of proteins identified (even only significant ones) not only causes challenges in the interpretation but also makes it difficult to integrate the outcomes with relatively few gene and enzyme stress markers. Therefore, it would be beneficial if further studies focused on integrating the interpretations of proteomic approaches with evaluations of the broad range of genes and biochemical parameters, not only with the stress-related genes and biomarkers but also with the more specific ones like immune response, neurodegenerative disorders and apoptosis.

5. Conclusion

In summary, we conducted proteomics, molecular and biochemical analysis multiapproach experiments to fill the gaps in the literature regarding the effects of insecticide-IMI exposure on aquatic nontarget organisms with the secondary aim of highlighting the complementary features of each method. The observed prominent outputs were the altered functions of the antioxidant, immune responses, and gene transcription proteins and their related pathways. Moreover, an apparent trend was observed toward the regulation mechanisms that risk the organism's survival in the long term by slowing down defense mechanisms such as apoptosis and ER stress. The results emphasize that these pathways and protein regulation may cause irreversible nervous system disorders and diseases such as cancer. We hope that these data will encourage future studies to explore defense mechanisms and focus on nontraditional new candidate biomarkers to obtain deeper insights into the exposure effects of insecticides. In this respect, we report that our observations revealed complementary features of these methods, thus underlining the importance of studying multiple approaches and considerably reflecting the crucial harmful effects of IMI. Therefore, we anticipate that this study may provide deeper insights for future ecotoxicological studies.

Ethics declaration

Experiments were performed with the approval of the welfare standards for care and use of the laboratory animals' ethics committee of Marmara University (Protocol code no: 67.2018.mar).

CRediT authorship contribution statement

Seyma Kizilkaya: Conceptualization, Methodology, Investigation, Writing – original draft, Visualization. **Gurler Akpinar:** Project administration, Supervision, Data curation. **Nuzhet Cenk Sesal:** Resources, Supervision. **Murat Kasap:** Resources, Supervision. **Baris Gokalsin:** Software, Methodology, Validation. **Figen Esin Kayhan:** Project administration, Supervision, Funding acquisition.

Declaration of competing interest

The authors declare that they have no known competing financial interests or personal relationships that could have appeared to influence the work reported in this paper.

Data availability

Data will be made available on request.

Acknowledgements

This project was supported by Marmara University Scientific Research Commission (BAPKO) with the project number FEN-C-DEP-110718-0409, and granted by The Scientific and Technological Research Council of Turkey (TUBITAK) BIDEP with the code 2211C. This study has been produced from the doctoral thesis of Seyma Kizilkaya. We thank to Dr. M.Gulsen Bal Albayrak and Dr. Mehmet Sarihan for their help in proteomics experiments, Serra Isik Tekler for assistance in molecular experiments and Dr. H. Eylul Esmer Duruel, Biol. S.Kardelen Dinc and S.Nazli Cagan Golcuk, in zebrafish maintenance and care.

Appendix A. Supplementary data

Supplementary data to this article can be found online at https://doi.org/10.1016/j.cbd.2023.101103.

References

Aebi, H., 1984. [13] Catalase in vitro. Methods Enzymol. 105, 121–126. https://doi.org/10.1016/S0076-6879(84)05016-3.

Akpinar, G., Yoneten, K.K., Kasap, M., Karaoz, E., 2021. Search for novel plasma membrane proteins as potential biomarkers in human mesenchymal stem cells derived from dental pulp, adipose tissue, bone marrow, and hair follicle. J. Membr. Biol. 254, 409–422. https://doi.org/10.1007/s00232-021-00190-1.

Albayrak, M.G.B., Simsek, T., Kasap, M., et al., 2022. Tissue proteome analysis revealed an association between cancer, immune system response, and the idiopathic granulomatous mastitis. Med. Oncol. 39, 238. https://doi.org/10.1007/s12032-022-01845-2.

Al-Dahmani, Z.M., Li, X., Wiggenhauser, L.M., Ott, H., Kruithof, P.D., Lunev, S.A., Batista, F., Luo, Y., Dolga, A.M., Morton, N.M., Groves, M.R., Kroll, J., van Goor, H., 2022. Thiosulfate sulfurtransferase prevents hyperglycemic damage to the zebrafish pronephros in an experimental model for diabetes. Sci. Rep. 12, 1–7. https://doi.org/10.1038/s41598-022-16320-1.

Anderson, J.C., Dubetz, C., Palace, V.P., 2015. Neonicotinoids in the Canadian aquatic environment: a literature review on current use products with a focus on fate, exposure, and biological effects. Sci. Total Environ. 505, 409–422. https://doi.org/10.1016/j.scitotenv.2014.09.090.

Araújo, M.J., Sousa, M.L., Fonseca, E., Felpeto, A.B., Martins, J.C., Vázquez, M., Mallo, N., Rodriguez-Lorenzo, L., Quarato, M., Pinheiro, I., Turkina, M.V., López-Mayán, J.J., Peña-Vázquez, E., Barciela-Alonso, M.C., Spuch-Calvar, M., Oliveira, M., Bermejo-Barrera, P., Cabaleiro, S., Espiña, B., Vasconcelos, V., Campos, A., 2022. Proteomics reveals multiple effects of titanium dioxide and silver nanoparticles in the metabolism of turbot, *Scophthalmus maximus*. Chemosphere 308. https://doi.org/10.1016/j.chemosphere.2022.136110.

Benli, P.P., Çelik, M., 2021. In vivo effects of neonicotinoid-sulfoximine insecticide sulfoxaflor on acetylcholinesterase activity in the tissues of zebrafish (*Danio rerio*). Toxics 9. https://doi.org/10.3390/toxics9040073.

Beutler, E., 1975. Glutathione peroxidase. In: Beutler, E. (Ed.), Cell Metabolism: A Manual of Biochemical Methods. Grune & Stratton, New York, pp. 71–73.

Bonmatin, J., Giorio, C., Girolami, V., Goulson, D., Kreutzweiser, D.P., 2015. Environmental Fate and Exposure; Neonicotinoids and Fipronil, pp. 35–67. https://doi.org/10.1007/s11356-014-3332-7.

Bresolin, T., De Freitas Rebelo, M., Dias Bainy, A.C., 2005. Expression of PXR, CYP3A and MDR1 genes in liver of zebrafish. Comp. Biochem. Physiol. C Toxicol. Pharmacol. 140, 403–407. https://doi.org/10.1016/j.cca.2005.04.003.

Bruckmann, F.S., Schnorr, C., Oviedo, L.R., Knani, S., Silva, L.F.O., Silva, W.L., Dotto, G. L., Bohn Rhoden, C.R., 2022. Adsorption and photocatalytic degradation of pesticides into nanocomposites: a review. Molecules 27. https://doi.org/10.3390/molecules27196261.

Bu, D., Luo, H., Huo, P., Wang, Z., Zhang, S., He, Z., Wu, Y., Zhao, L., Liu, J., Guo, J., Fang, S., Cao, W., Yi, L., Zhao, Y., Kong, L., 2021. KOBAS-i: intelligent prioritization and exploratory visualization of biological functions for gene enrichment analysis. Nucleic Acids Res. 49, W317–W325. https://doi.org/10.1093/nar/gkab447.

Carbon, S., Douglass, E., Good, B.M., Unni, D.R., Harris, N.L., Mungall, C.J., Basu, S., Chisholm, R.L., Dodson, R.J., Hartline, E., Fey, P., Thomas, P.D., Albou, L.P., Ebert, D., Kesling, M.J., Mi, H., Muruganujan, A., Huang, X., Mushayahama, T.,

LaBonte, S.A., Siegele, D.A., Antonazzo, G., Attrill, H., Brown, N.H., Garapati, P., Marygold, S.J., Trovisco, V., dos Santos, G., Falls, K., Tabone, C., Zhou, P., Goodman, J.L., Strelets, V.B., Thurmond, J., Garmiri, P., Ishtiaq, R., Rodríguez-López, M., Acencio, M.L., Kuiper, M., Lægreid, A., Logie, C., Lovering, R.C., Kramarz, B., Saverimuttu, S.C.C., Pinheiro, S.M., Gunn, H., Su, R., Thurlow, K.E., Chibucos, M., Giglio, M., Nadendla, S., Munro, J., Jackson, R., Duesbury, M.J., Del-Toro, N., Meldal, B.H.M., Paneerselvam, K., Perfetto, L., Porras, P., Orchard, S., Shrivastava, A., Chang, H.Y., Finn, R.D., Mitchell, A.L., Rawlings, N.D., Richardson, L., Sangrador-Vegas, A., Blake, J.A., Christie, K.R., Dolan, M.E., Drabkin, H.J., Hill, D.P., Ni, L., Sitnikov, D.M., Harris, M.A., Oliver, S.G., Rutherford, K., Wood, V., Hayles, J., Bähler, J., Bolton, E.R., de Pons, J.L., Dwinell, M.R., Hayman, G.T., Kaldunski, M.L., Kwitek, A.E., Laulederkind, S.J.F., Plasterer, C., Tutaj, M.A., Vedi, M., Wang, S.J., D'Eustachio, P., Matthews, L., Balhoff, J.P., Aleksander, S.A., Alexander, M.J., Cherry, J.M., Engel, S.R., Gondwe, F., Karra, K., Miyasato, S.R., Nash, R.S., Simison, M., Skrzypek, M.S., Weng, S., Wong, E.D., Feuermann, M., Gaudet, P., Morgat, A., Bakker, E., Berardini, T.Z., Reiser, L., Subramaniam, S., Huala, E., Arighi, C.N., Auchincloss, A., Axelsen, K., Argoud-Puy, G., Bateman, A., Blatter, M.C., Boutet, E., Bowler, E., Breuza, L., Bridge, A., Britto, R., Bye-A-Jee, H., Casas, C.C., Coudert, E., Denny, P., Es-Treicher, A., Famiglietti, M.L., Georghiou, G., Gos, A.N., Gruaz-Gumowski, N., Hatton-Ellis, E., Hulo, C., Ignatchenko, A., Jungo, F., Laiho, K., Le Mercier, P., Lieberherr, D., Lock, A., Lussi, Y., MacDougall, A., Ma-Grane, M., Martin, M.J., Masson, P., Natale, D.A., Hyka-Nouspikel, N., Orchard, S., Pedruzzi, I., Pourcel, L., Poux, S., Pundir, S., Rivoire, C., Speretta, E., Sundaram, S., Tyagi, N., Warner, K., Zaru, R., Wu, C.H., Diehl, A.D., Chan, J.N., Grove, C., Lee, R.Y.N., Muller, H.M., Raciti, D., van Auken, K., Sternberg, P.W., Berriman, M., Paulini, M., Howe, K., Gao, S., Wright, A., Stein, L., Howe, D.G., Toro, S., Westerfield, M., Jaiswal, P., Cooper, L., Elser, J., 2021. The gene ontology resource: enriching a GOld mine. Nucleic Acids Res. 49, D325–D334. https://doi.org/10.1093/nar/gkaa1113.

Chang, Y., Mao, L., Zhang, L., Zhang, Y., Jiang, H., 2020. Combined toxicity of imidacloprid, acetochlor, and tebuconazole to zebrafish (*Danio rerio*): acute toxicity and hepatotoxicity assessment. Environ. Sci. Pollut. Res. Int. https://doi.org/10.1007/s11356-020-07653-3.

Chen, M., Zhai, J., Liu, Y., Xue, B., Hu, Jiahuan, Cheng, X., Li, J., Hu, Jingsheng, Li, B., 2018. Molecular cloning and characterization of C1 tetrahydrofolate (C1-THF) synthase in *Bombyx mori*, silkworm. Gene 663, 25–33. https://doi.org/10.1016/j.gene.2018.04.037.

Chen, Q.L., Sun, Y.L., Liu, Z.H., Li, Y.W., 2017. Sex-dependent effects of subacute mercuric chloride exposure on histology, antioxidant status and immune-related gene expression in the liver of adult zebrafish (*Danio rerio*). Chemosphere 188, 1–9. https://doi.org/10.1016/j.chemosphere.2017.08.148.

Collodet, C., Foretz, M., Deak, M., Bultot, L., Metairon, S., Viollet, B., Lefebvre, G., Raymond, F., Parisi, A., Civiletto, G., Gut, P., Descombes, P., Sakamoto, K., 2019. AMPK promotes induction of the tumor suppressor FLCN through activation of TFEB independently of mTOR. FASEB J. 33, 12374–12391. https://doi.org/10.1096/fj.201900841R.

Colombo, V., Mohr, S., Berghahn, R., Pettigrove, V.J., 2013. Structural changes in a macrozoobenthos assemblage after imidacloprid pulses in aquatic field-based microcosms. Arch. Environ. Contam. Toxicol. 65, 683–692. https://doi.org/10.1007/s00244-013-9940-2.

Creusot, N., Garoche, C., Grimaldi, M., Boulahtouf, A., Chiavarina, B., Bourguet, W., Balaguer, P., 2021. A comparative study of human and zebrafish Pregnane X receptor activities of pesticides and steroids using in vitro reporter gene assays. Front. Endocrinol. (Lausanne). 12, 1–10. https://doi.org/10.3389/fendo.2021.665521.

Dong, W.Q., Sun, H.J., Zhang, Y., Lin, H.J., Chen, J.R., Hong, H.C., 2018. Impact on growth, oxidative stress, and apoptosis-related gene transcription of zebrafish after exposure to low concentration of arsenite. Chemosphere 211, 648–652. https://doi.org/10.1016/j.chemosphere.2018.08.010.

Ellman, G.L., Courtney, K.D., Andres, V., Featherstone, R.M., 1961. A new and rapid colorimetric determination of acetylcholinesterase activity. Biochem. Pharmacol. 7, 88–95. https://doi.org/10.1016/0006-2952(61)90145-9.

Esin Kayhan, F., Kaymak, G., Esmer Duruel, H.E., Kızılkaya, Ş., 2019. Some oxidative stress parameters in heart tissue of zebrafish (*Danio reiro*) caused by mancozeb. Ege J. Fish. Aquat. Sci. 36, 325–328. https://doi.org/10.12714/egejfas.36.4.02.

Esmer Duruel, H., Kayhan, F., 2021. Evaluating the biochemical effects of sublethal exposure to glufosinate-ammonium on model organism Zebrafish (Danio rerio) tissues. Fresen. Environ. Bull. 30, 12558–12564.

Gao, Y., Lee, H., Lee, S., Kim, K.T., 2022. Type 2 diabetes induced by changes in proteomic profiling of zebrafish chronically exposed to a mixture of organochlorine pesticides at low concentrations. Int. J. Environ. Res. Public Health 19. https://doi.org/10.3390/ijerph19094991.

Glaberman, S., Padilla, S., Barron, M.G., 2017. Evaluating the zebrafish embryo toxicity test for pesticide hazard screening. Environ. Toxicol. Chem. 36, 1221–1226. https://doi.org/10.1002/etc.3641.

Groh, K.J., Suter, M.J.F., 2015a. Stressor-induced proteome alterations in zebrafish: a meta-analysis of response patterns. Aquat. Toxicol. 159, 1–12. https://doi.org/10.1016/j.aquatox.2014.11.013.

Groh, K.J., Suter, M.J.F., 2015b. Stressor-induced proteome alterations in zebrafish: a meta-analysis of response patterns. Aquat. Toxicol. 159, 1–12. https://doi.org/10.1016/j.aquatox.2014.11.013.

Guerra, L.J., do Amaral, A.M.B., de Quadros, V.A., da Luz Fiuza, T., Rosemberg, D.B., Prestes, O.D., Zanella, R., Clasen, B., Loro, V.L., 2021. Biochemical and behavioral responses in zebrafish exposed to imidacloprid oxidative damage and antioxidant responses. Arch. Environ. Contam. Toxicol. 81, 255–264. https://doi.org/10.1007/s00244-021-00865-9.

Hellemans, J., Mortier, G., De Paepe, A., Speleman, F., Vandesompele, J., 2008. qBase relative quantification framework and software for management and automated analysis of real-time quantitative PCR data. Genome Biol. 8 https://doi.org/10.1186/gb-2007-8-2-r19.

Hladik, M.L., Corsi, S.R., Kolpin, D.W., Baldwin, A.K., Blackwell, B.R., Cavallin, J.E., 2018. Year-round presence of neonicotinoid insecticides in tributaries to the Great Lakes, USA. Environ. Pollut. https://doi.org/10.1016/j.envpol.2018.01.013.

Hong, C., Choi, S.H., Kwak, M., Jeong, B., Ko, J., Park, H.J., Choi, S., Jun, J.Y., So, I., 2020. TRPC5 channel instability induced by depalmitoylation protects striatal neurons against oxidative stress in Huntington's disease. Biochim. Biophys. Acta Mol. Cell Res. 1867, 118620 https://doi.org/10.1016/j.bbamcr.2019.118620.

Horzmann, K.A., Reidenbach, L.S., Thanki, D.H., Winchester, A.E., Qualizza, B.A., Ryan, G.A., Egan, K.E., Hedrick, V.E., Sobreira, T.J.P., Peterson, S.M., Weber, G.J., Wirbisky-Hershberger, S.E., Sepúlveda, M.S., Freeman, J.L., 2018. Embryonic atrazine exposure elicits proteomic, behavioral, and brain abnormalities with developmental time specific gene expression signatures. J. Proteome 186, 71–82. https://doi.org/10.1016/j.jprot.2018.07.006.

Huang, Y., Ma, J., Meng, Y., Wei, Y., Xie, S., Jiang, P., Wang, Z., Chen, X., Liu, Z., Zhong, K., Cao, Z., Liao, X., Xiao, J., Lu, H., 2020. Exposure to Oxadiazon-Butachlor causes cardiac toxicity in zebrafish embryos. Environ. Pollut. 265 https://doi.org/10.1016/j.envpol.2020.114775.

Jiao, Y., Tao, Y., Yang, Y., Diogene, T., Yu, H., He, Z., Han, W., Chen, Z., Wu, P., Zhang, Y., 2020. Monobutyl phthalate (MBP) can dysregulate the antioxidant system and induce apoptosis of zebrafish liver. Environ. Pollut. 257, 113517 https://doi.org/10.1016/j.envpol.2019.113517.

Kandel, R.R., Neal, S.E., 2020. The role of rhomboid superfamily members in protein homeostasis: mechanistic insight and physiological implications. Biochim. Biophys. Acta Mol. Cell Res. 1867, 1–20. https://doi.org/10.1016/j.bbamcr.2020.118793.

Kaokhum, N., Pinto-Fernández, A., Wilkinson, M., Kessler, B.M., Ismail, H.M., 2022. The mechano-ubiquitinome of articular cartilage: differential ubiquitination and activation of a group of ER-associated DUBs and ER stress regulators. Mol. Cell. Proteomics 100419. https://doi.org/10.1016/j.mcpro.2022.100419.

Kayhan, F.E., Esmer Duruel, H.E., Kizilkaya, S., Dinc, S.K., Kaymak, G., Akbulut, C., Yon Ertug, N.D., 2020. Toxic effects of herbicide tribenuron-methyl on liver tissue of zebrafish (*Danio rerio*). Fresenius Environ. Bull. 29, 11175–11179.

Kwon, Y.S., Park, C.-B., Lee, S.-M., Zee, S., Kim, G.-E., Kim, Y.-J., Sim, H.-J., Kim, J.-H., Seo, J.-S., 2022. Proteomic analysis of zebrafish (*Danio rerio*) embryos exposed to benzyl benzoate. Environ. Sci. Pollut. Res. https://doi.org/10.1007/s11356-022-24081-7.

Ledwożyw, A., Michalak, J., Stępień, A., Kadziołka, A., 1986. The relationship between plasma triglycerides, cholesterol, total lipids and lipid peroxidation products during human atherosclerosis. Clin. Chim. Acta 155, 275–283. https://doi.org/10.1016/0009-8981(86)90247-0.

Li, L., Liu, M., Zhang, Z., Zhang, W., Liu, N., Sheng, X., Wei, P., 2019. Derlin1 functions as an oncogene in cervical cancer via AKT/mTOR signaling pathway. Biol. Res. 52, 8. https://doi.org/10.1186/s40659-019-0215-x.

Li, M., Yu, T., Lai, J., Han, X., Hu, J., Deng, Z., Li, D., Ye, Z., Wang, S., Hu, C., Xu, X., 2021. Ethoprophos induces cardiac toxicity in zebrafish embryos. Ecotoxicol. Environ. Saf. 228, 113029 https://doi.org/10.1016/j.ecoenv.2021.113029.

Li, Q., Jiang, W., Wan, Z., Ni, Y., Lei, L., Wei, J., 2020. Polyphyllin I attenuates pressure over-load induced cardiac hypertrophy via inhibition of Wnt/β-catenin signaling pathway. Life Sci. 252, 117624 https://doi.org/10.1016/j.lfs.2020.117624.

Li, X., Wang, Q., Wang, C., Yang, Z., Wang, Jinhua, Zhu, L., Zhang, D., Wang, Jun, 2022. Ecotoxicological response of zebrafish liver (Danio rerio) induced by di-(2-ethylhexyl) phthalate. Ecol. Indic. 143, 109388. doi:https://doi.org/10.1016/j.ecolind.2022.109388.

Lin, H.D., Hsu, L.S., Chien, C.C., Chen, S.C., 2018. Proteomic analysis of ametryn toxicity in zebrafish embryos. Environ. Toxicol. 33, 579–586. https://doi.org/10.1002/tox.22546.

Luo, T., Wang, X., Jin, Y., 2021a. Low concentrations of imidacloprid exposure induced gut toxicity in adult zebrafish (*Danio rerio*). Comp. Biochem. Physiol. C Toxicol. Pharmacol. 241, 108972 https://doi.org/10.1016/j.cbpc.2020.108972.

Luo, T., Wang, X., Jin, Y., 2021b. Low concentrations of imidacloprid exposure induced gut toxicity in adult zebrafish (*Danio rerio*). Comp. Biochem. Physiol. C 241, 108972. https://doi.org/10.1016/j.cbpc.2020.108972.

Luo, T., Weng, Y., Huang, Z., Zhao, Y., Jin, Y., 2021c. Combined hepatotoxicity of imidacloprid and microplastics in adult zebrafish: endpoints at gene transcription. Comp. Biochem. Physiol. C Toxicol. Pharmacol. 246, 109043 https://doi.org/10.1016/j.cbpc.2021.109043.

McGrath, P., Li, C.Q., 2008. Zebrafish: a predictive model for assessing drug-induced toxicity. Drug Discov. Today. https://doi.org/10.1016/j.drudis.2008.03.002.

Morrissey, C.A., Mineau, P., Devries, J.H., Sanchez-bayo, F., Liess, M., Cavallaro, M.C., Liber, K., 2015. Neonicotinoid contamination of global surface waters and associated risk to aquatic invertebrates: a review. Environ. Int. 74, 291–303. https://doi.org/10.1016/j.envint.2014.10.024.

Ni, H., Peng, L., Gao, X., Ji, H., Ma, J., Li, Y., Jiang, S., 2019. Effects of maduramicin on adult zebrafish (*Danio rerio*): acute toxicity, tissue damage and oxidative stress. Ecotoxicol. Environ. Saf. 168, 249–259. https://doi.org/10.1016/j.ecoenv.2018.10.040.

Nyman, A., Hintermeister, A., Schirmer, K., Ashauer, R., 2013. The insecticide imidacloprid causes mortality of the freshwater amphipod *Gammarus pulex* by interfering with feeding behavior. PLoS One 8. https://doi.org/10.1371/journal.pone.0062472.

OECD, 1992. Oslo Manual — 1st Edition. Proposed Guidelines for Collecting and Interpreting Technological Innovation Data. OECD, Paris.

Piña, B., Ziv, T., Faria, M., Ben-Lulu, S., Prats, E., Arick, M.A., Gomez-Canela, C., Garcıa-Reyero, N., Admon, A., Raldua, D., 2019. Multiomic analysis of zebrafish models of acute organophosphorus poisoning with different severity. Toxicol. Sci. 171, 211–220. https://doi.org/10.1093/toxsci/kfz133.

Queiroz, L.G., do Prado, C.C.A., de Almeida, É.C., Dörr, F.A., Pinto, E., da Silva, F.T., de Paiva, T.C.B., 2021. Responses of aquatic nontarget organisms in experiments simulating a scenario of contamination by imidacloprid in a freshwater environment. Arch. Environ. Contam. Toxicol. 80, 437–449. https://doi.org/10.1007/s00244-020-00782-3.

Raudvere, U., Kolberg, L., Kuzmin, I., Arak, T., Adler, P., Peterson, H., Vilo, J., 2019. G: Profiler: a web server for functional enrichment analysis and conversions of gene lists (2019 update). Nucleic Acids Res. 47, W191–W198. https://doi.org/10.1093/nar/gkz369.

Reinwald, H., Alvincz, J., Salinas, G., Schäfers, C., Hollert, H., Eilebrecht, S., 2022. Toxicogenomic profiling after sublethal exposure to nerve- and muscle-targeting insecticides reveals cardiac and neuronal developmental effects in zebrafish embryos. Chemosphere 291. https://doi.org/10.1016/j.chemosphere.2021.132746.

Scheil, V., Köhler, H.R., 2009. Influence of nickel chloride, chlorpyrifos, and imidacloprid in combination with different temperatures on the embryogenesis of the zebrafish *Danio rerio*. Arch. Environ. Contam. Toxicol. 56, 238–243. https://doi.org/10.1007/s00244-008-9192-8.

Shukla, S., Jhamtani, R.C., Dahiya, M.S., Agarwal, R., 2017a. Oxidative injury caused by individual and combined exposure of neonicotinoid, organophosphate and herbicide in zebrafish. Toxicol. Rep. 4, 240–244. https://doi.org/10.1016/j.toxrep.2017.05.002.

Shukla, S., Jhamtani, R.C., Dahiya, M.S., Agarwal, R., 2017b. Oxidative injury caused by individual and combined exposure of neonicotinoid, organophosphate and herbicide in zebrafish. Toxicol. Rep. https://doi.org/10.1016/j.toxrep.2017.05.002.

Simmons, D.B.D., Cowie, A.M., Koh, J., Sherry, J.P., Martyniuk, C.J., 2019. Label-free and iTRAQ proteomics analysis in the liver of zebrafish (*Danio rerio*) following dietary exposure to the organochlorine pesticide dieldrin. J. Proteome 202, 103362. https://doi.org/10.1016/j.jprot.2019.04.012.

Simsek, H.U., Albayrak, M.G.B., Kasap, M., Simsek, T., Akpinar, G., Guler, S.A., Canturk, N.Z., 2022. Elucidation of the changes occurring at the proteome level in ovaries of high-fat diet-induced obese rats. Cell Biochem. Funct. 40, 278–297. https://doi.org/10.1002/cbf.3693.

Smit, C.E., De Jong, F.M.W., 2014. Human and ecological risk assessment. In: Ecotoxicity of Imidacloprid to Aquatic Organisms: Derivation of Water Quality Standards for Peak and Long-term Exposure, pp. 37–41. https://doi.org/10.1080/10807039.2014.964071.

Sposito, J.C.V., Montagner, C.C., Casado, M., Navarro-Martín, L., Jut Solórzano, J.C., Piña, B., Grisolia, A.B., 2018. Emerging contaminants in Brazilian rivers: occurrence and effects on gene expression in zebrafish (*Danio rerio*) embryos. Chemosphere 209, 696–704. https://doi.org/10.1016/j.chemosphere.2018.06.046.

Struger, J., Grabuski, J., Cagampan, S., Sverko, E., McGoldrick, D., Marvin, C.H., 2017. Factors influencing the occurrence and distribution of neonicotinoid insecticides in surface waters of southern Ontario, Canada. Chemosphere 169, 516–523. https://doi.org/10.1016/j.chemosphere.2016.11.036.

Sürmen, M.G., Sürmen, S., Cansız, D., Ünal, İ., Üstündağ, Ü.V., Alturfan, A.A., Emekli-Alturfan, E., 2021. Quantitative phosphoproteomics to resolve the cellular responses to octanoic acid in rotenone exposed zebrafish. J. Food Biochem. 45, 1–17. https://doi.org/10.1111/jfbc.13923.

Thunnissen, N.W., Lautz, L.S., van Schaik, T.W.G., Hendriks, A.J., 2020. Ecological risks of imidacloprid to aquatic species in the Netherlands: measured and estimated concentrations compared to species sensitivity distributions. Chemosphere 254, 126604. https://doi.org/10.1016/j.chemosphere.2020.126604.

Tierbach, A., Groh, K.J., Schönenberger, R., Schirmer, K., Suter, M.J.F., 2018. Glutathione S-transferase protein expression in different life stages of zebrafish (*Danio rerio*). Toxicol. Sci. 162, 702–712. https://doi.org/10.1093/toxsci/kfx293.

Tišler, T., Jemec, A., Mozetic, B., 2009. Hazard identification of imidacloprid to aquatic environment. Chemosphere 76, 907–914. https://doi.org/10.1016/j.chemosphere.2009.05.002.

Topal, A., Alak, G., Ozkaraca, M., Yeltekin, A.C., Comaklı, S., Acıl, G., Kokturk, M., Atamanalp, M., 2017a. Neurotoxic responses in brain tissues of rainbow trout exposed to imidacloprid pesticide: assessment of 8-hydroxy-2-deoxyguanosine activity, oxidative stress and acetylcholinesterase activity. Chemosphere 175, 186–191. https://doi.org/10.1016/j.chemosphere.2017.02.047.

Topal, A., Alak, G., Ozkaraca, M., Yeltekin, A.C., Comaklı, S., Acıl, G., Kokturk, M., Atamanalp, M., 2017b. Neurotoxic responses in brain tissues of rainbow trout exposed to imidacloprid pesticide: assessment of 8-hydroxy-2-deoxyguanosine activity, oxidative stress and acetylcholinesterase activity. Chemosphere 175, 186–191. https://doi.org/10.1016/j.chemosphere.2017.02.047.

Truong, T.H., Carroll, K.S., 2013. Redox regulation of protein kinases. Crit. Rev. Biochem. Mol. Biol. 48, 332–356. https://doi.org/10.3109/10409238.2013.790873.

Valdés, A., Bitzios, A., Kassa, E., Shevchenko, G., Falk, A., Malmström, P.U., Dragomir, A., Segersten, U., Lind, S.B., 2021. Proteomic comparison between different tissue preservation methods for identification of promising biomarkers of urothelial bladder cancer. Sci. Rep. 11, 1–12. https://doi.org/10.1038/s41598-021-87003-6.

Van Dijk, T.C., Van Staalduinen, M.A., Van der Sluijs, J.P., 2013. Macro-Invertebrate decline in surface water polluted with imidacloprid. PLoS ONE 8 (5), e62374. https://doi.org/10.1371/journal.pone.0062374.

Vandesompele, J., De Preter, K., Pattyn, Ilip, Poppe, B., Van Roy, N., De Paepe, A., Speleman, Rank, 2002. Accurate normalization of real-time quantitative RT-PCR data by geometric averaging of multiple internal control genes. Genome Biol. 3 (7), 0034.1–0034.11.

Vieira, L.R., Hissa, D.C., de Souza, T.M., Chayenne, A.S., Evaristo, J.A.M., Nogueira, F.C. S., Carvalho, A.F.U., Farias, D.F., 2020. Proteomics analysis of zebrafish larvae exposed to 3,4-dichloroaniline using the fish embryo acute toxicity test. Environ. Toxicol. 35, 849–860. https://doi.org/10.1002/tox.22921.

Wang, H., Lin, C., Yao, J., Shi, H., Zhang, C., Wei, Q., Lu, Y., Chen, Z., Xing, G., Cao, X., 2019. Deletion of OSBPL2 in auditory cells increases cholesterol biosynthesis and drives reactive oxygen species production by inhibiting AMPK activity. Cell Death Dis. 10 https://doi.org/10.1038/s41419-019-1858-9.

Wang, Y., Yang, G., Dai, D., Xu, Z., Cai, L., Wang, Q., Yu, Y., 2017. Individual and mixture effects of five agricultural pesticides on zebrafish (*Danio rerio*) larvae. Environ. Sci. Pollut. Res. 24, 4528–4536. https://doi.org/10.1007/s11356-016-8205-9.

Wu, S., Li, X., Liu, X., Yang, G., An, X., Wang, Q., Wang, Y., 2018a. Joint toxic effects of triazophos and imidacloprid on zebrafish (*Danio rerio*). Environ. Pollut. 235, 470–481. https://doi.org/10.1016/j.envpol.2017.12.120.

Wu, S., Li, X., Liu, X., Yang, G., An, X., Wang, Q., Wang, Y., 2018b. Joint toxic effects of triazophos and imidacloprid on zebrafish (*Danio rerio*). Environ. Pollut. 235, 470–481. https://doi.org/10.1016/j.envpol.2017.12.120.

Xie, M., Hao, Q., Xia, R., Olsen, R.E., Ringø, E., Yang, Y., Zhang, Z., Ran, C., Zhou, Z., 2022. Nuclease-treated stabilized fermentation product of *Cetobacterium somerae* improves growth, non-specific immunity, and liver health of zebrafish (*Danio rerio*). Front. Nutr. 9, 1–11. https://doi.org/10.3389/fnut.2022.918327.

Yanar, S., Kasap, M., Kanli, A., Akpinar, G., Sarihan, M., J., 2023. Proteomics analysis of meclofenamic acid-treated small cell lung carcinoma cells revealed changes in cellular energy metabolism for cancer cell survival. Biochem. Mol. Toxicol. 37, e23289 https://doi.org/10.1002/jbt.23289.

Yoshida, H., 1989. Hydrolysis of NTN 33898. Miles Inc. (Mobay) Premise Termiticide. Study No. 99708. DPR Vol. 51950-0027 # 119533.

Zancan, I., Bellesso, S., Costa, R., Salvalaio, M., Stroppiano, M., Hammond, C., Argenton, F., Filocamo, M., Moro, E., 2015. Glucocerebrosidase deficiency in zebrafish affects primary bone ossification through increased oxidative stress and reduced Wnt/β-catenin signaling. Hum. Mol. Genet. 24, 1280–1294. https://doi.org/10.1093/hmg/ddu538.

Zhang, H.C., Ma, K.X., Yang, Y.J., Shi, C.Y., Chen, G.W., Liu, D.Z., 2018. Molecular cloning, characterization, expression and enzyme activity of catalase from planarian *Dugesia japonica* in response to environmental pollutants. Ecotoxicol. Environ. Saf. 165, 88–95. https://doi.org/10.1016/j.ecoenv.2018.08.083.

Zhang, J., Liu, L., Ren, L., Feng, W., Lv, P., Wu, W., Yan, Y., 2017. The single and joint toxicity effects of chlorpyrifos and beta-cypermethrin in zebrafish (*Danio rerio*) early life stages. J. Hazard. Mater. 334, 121–131. https://doi.org/10.1016/j.jhazmat.2017.03.055.

Zhang, J.G., Ma, D.D., Xiong, Q., Qiu, S.Q., Huang, G.Y., Shi, W.J., Ying, G.G., 2021. Imidacloprid and thiamethoxam affect synaptic transmission in zebrafish. Ecotoxicol. Environ. Saf. 227, 112917 https://doi.org/10.1016/j.ecoenv.2021.112917.

Zhu, H., Gao, M., Sun, W., Liu, H., Xu, S., Li, X., 2023. ROS/ER stress contributes to trimethyltin chloride-mediated hepatotoxicity; tea polyphenols alleviate apoptosis and immunosuppression. Comp. Biochem. Physiol. C Toxicol. Pharmacol. 263, 109505 https://doi.org/10.1016/j.cbpc.2022.109505.